DESIGN OF AN FM-CW RADAR ALTIMETER

A THESIS SUBMITTED TO
THE GRADUATE SCHOOL OF NATURAL AND APPLIED SCIENCES
OF
MIDDLE EAST TECHNICAL UNIVERSITY

BY

YAŞAR BARIŞ YETKİL

IN PARTIAL FULFILLMENT OF THE REQUIREMENTS
FOR
THE DEGREE OF MASTER OF SCIENCE
IN
ELECTRICAL AND ELECTRONICS ENGINEERING

DECEMBER 2005

Approval of the Graduate School of Natural and Applied Sciences.

_____

Prof. Dr. Canan Özgen

Director

I certify that this thesis satisfies all the requirements as a thesis for the degree of Master of Science.

_____

Prof. Dr. İsmet Erkmen

Head of Department

This is to certify that we have read this thesis and that in our opinion it is fully adequate, in scope and quality, as a thesis for the degree of Master of Science.

_____   _____

Prof. Dr. Yalçın Tanık   Assoc. Prof. Dr. Şimşek Demir

Co-Supervisor   Supervisor

Examining Committee Members

Prof. Dr. Altunkan Hızal	(METU, EE)	_____
Assoc. Prof. Dr. Şimşek Demir	(METU, EE)	_____
Prof. Dr. Yalçın Tanık	(METU, EE)	_____
Assoc. Prof. Dr. Seyit Sencer Koç	(METU, EE)	_____
Mr. Mehmet Birol Özden	(TAPASAN)	_____

Hereby I declare that all information in this document has been obtained and presented in accordance with academic rules and ethical conduct. I also declare that, as required by these rules and conduct, I have fully cited and referenced all material and results that are not original to this work.

Name, Last Name   : Yaşar Barış Yetkil

Signature   :

ABSTRACT

DESIGN OF AN FM-CW RADAR ALTIMETER

Yetkil, Yaşar Barış

MS., Department of Electrical and Electronics Engineering

Supervisor: Assoc. Prof. Dr. Şimşek Demir

Co-Supervisor: Prof. Dr. Yalçın Tanık

December 2005, 72 pages

Frequency modulated continuous wave (FM-CW) radar altimeters are used in civil and military applications. Proximity fuses, automatic cruise control systems of cars, radar altimeter of planes are examples to these applications.

The goal of this thesis is to present a method for altitude determination using an FM-CW radar. For this purpose principles of radars and FM-CW systems are studied and related subjects are inspected. After this inspection, algorithms for altitude determination are evaluated. Consequently signal detection and processing methods are proposed to build an altitude determining algorithm. Also an analytical test environment for altitudes between 100 m and 4000 m is developed in computer as a result of researches. Test environment simulated the performance of altitude determining algorithm and *FM-CW Radar Altimeter*. The hardware is designed and implemented accordingly.

Keywords: FM-CW, altimeter, altitude determining algorithm

ÖZ

FM-CW YÜKSEKLİK ÖLÇER RADAR TASARIMI

Yetkil, Yaşar Barış

Yüksek Lisans, Elektrik ve Elektronik Mühendisliği Bölümü

Tez Yöneticisi   : Doç. Dr. Şimşek Demir

Ortak Tez Yöneticisi   : Prof. Dr. Yalçın Tanık

Aralık 2005, 72 sayfa

Frekans kiplenmiş sürekli dalga (FM-CW) yükseklik ölçer radarı, askeri amaçlı yaklaşım tapası, arabalarda denenen otomatik yolculuk kontrol sistemi ve uçaklarda bulunan yükseklik ölçer gibi birçok uygulamada kullanılmaktadır.

Bu çalışmanın amacı FM-CW radarı kullanarak yükseklik ölçümü için bir yöntem geliştirmektir. Bu amaçla radarın ve FM-CW sistemlerin çalışma prensibi gözden geçirilmiş ve yükseklik ölçümünde etkili olan olaylar incelenmiştir. Bu incelemenin ardından yükseklik ölçümünde kullanılan yöntemler değerlendirilmiştir. Değerlendirme sonucunda yükseklik ölçen algoritma oluşturmak amacı ile sinyal tespit etme ve işleme yolu önerilmiştir. Ayrıca araştırmalar sonucunda 100 m ile 4000 m arasında, algoritmanın sınanabileceği analitik çalışma yapılmıştır. Bu çalışmaya göre yükseklik ölçen algoritmanın ve *FM-CW Yükseklik Ölçer Radar*ın performansı bilgisayar ortamında test edilmiş, buna göre sistemin donanımı tasarlanmıştır ve gerçeklenmiştir.

Anahtar Kelimeler: FM-CW, Yükseklik Ölçer, Yükseklik Ölçen Algoritma

To the Memory of My Father

ACKNOWLEDGMENTS

TABLE OF CONTENTS

LIST OF TABLES

LIST OF FIGURES

CHAPTER 1

INTRODUCTION

1.1   Radar Introduction

The word radar is coined from the initial letters of the phrase; **Ra**dio **D**etection **a**nd **R**anging. Radar is used for remote sensing of objects, land, etc.. This is accomplished via sending an electromagnetic wave in various frequencies (Appendix A) and receiving the reflection from the object which is very similar to sound echo reflected back from a valley. Radar is designed to see through darkness, fog, rain and snow. It is also used to measure range and speed. According to Skolnik [1] these are the most important attributes of radar. However, radar is evolved over a hundred years of work and experience.

1.1.1   Radar History

Radar history dates back to James Clerk Maxwell. In 1865 the English physicist developed his electromagnetic light theory. In 1887 German Physicist Heinrich Hertz began experimenting with radio waves. James Clerk Maxwell predicted the existence of electromagnetic waves but it was Heinrich Hertz who first generated and detected electromagnetic waves experimentally.

By the 1900s a German engineer, Christian Huelsmeyer proposed the use of radio echoes to avoid collisions. He invented a device he called the telemobiloscope, which consisted of a simple spark gap aimed using a funnel-shaped metal antenna. When a reflection was seen by the two straight antennas attached to the receiver, a

bell sounded. The system was very simple; it could detect shipping accurately up to about 3 km. However it was far away from civil and military applications.

In 1922 A. H. Taylor and L. C. Young from USA Naval Research Laboratory (NRL) located a wooden ship for the first time.

During World War II (WWII) significant achievements were obtained on radars. Shortly before the outbreak of World War II several radar stations known as Chain Home (CH) were constructed in the south of England [2]. CH successfully operated during Battle of Britain and German bomber aircrafts detected over sea with the aid of radars. The air raids detected earlier and interceptors guided accordingly to prevent those raids.

At the end of the WWII, most of today's technologies had already been put to use, although they relied on contemporary technical means [3].

Today, besides military applications, radars are widely used from speed detection in highways to obstacle avoidance for parking, and from whether casting to measurement of Antarctic ice sheet thickness from satellites. Further information can be obtained from [1] - [3] on radar history.

1.2   FM-CW Radar Introduction

FM-CW radar is a form of radar. In this radar the transmitted energy is frequency modulated. The advantage of FM-CW technique is its ability to determine height very accurately over a large surface. Another advantage is continuous wave transmission, which allows accurate relative height measurement with low power outputs. The main disadvantage is the coupling of harmonics of modulation frequency to receiver (leakage from the transmitter to receiver) and nonlinearities in the modulating signal.

1.2.1 FM-CW Radar History

The first practical model of the FM-CW radar altimeter was developed by the Western Electric Company in 1938, although the principles of altitude determination using radio-wave reflections were known ten years earlier in 1928 [4].

FM-CW was applied to the measurement of the height of the ionosphere in the 1920s [5] and as an aircraft altimeter in the 1930s [6] as Skolnik references. However the improvements in pulsed radar after the end of 1930s reduced the interest on FM-CW radar. But recently, the requirements in portable, small, low power and accurate range detectors gave rise to FM-CW studies according to [7].

Today, FM-CW radar is widely used from park sensors in the cars to adaptive cruise control (ACC) [8] and from altimeters in planes to surface penetrating radars to measure ice thickness [9]. Neverthless the military applications takes the first place amongst the FM-CW applications with altimeters and proximity fuses.

1.3 Thesis Overview

The goal of this thesis is to present a method for altitude determination. In order to do this there are various ways such as sound, optics and air pressure difference.

In this thesis radar approach will be inspected and FM-CW technique will be used. For this purpose firstly, an introduction on radar and FM-CW radar is given.

Later in Chapter 2, basic operation and basic equation of radar will be given. Following *radar background* section, *FM-CW radar background* and basic parameters will be given. After *FM-CW radar background*, *radar cross section* (RCS) will be inspected in detail. Later, with *radar background* and *RCS*, impulse response and back scattering from rough surfaces will be discussed. This impulse

3

response will be improved with the statistical channel response to obtain statistical properties between measurement windows. Finally, signal processing parameters will be discussed.

In Chapter 3, simulation environment and simulation of the FM-CW radar altimeter will be discussed. An algorithm for altitude determination will be presented and performance will be discussed.

In Chapter 4, electronic circuits of FM-CW radar altimeter is inspected. System parameters, block diagrams, calculations and operation results of the FM-CW radar altimeter will be given.

Finally in Chapter 5, the work will be summarized and future improvements will be discussed.

CHAPTER 2

BACKGROUND MATERIALS

2.1   Radar Background [1], [10]

2.1.1   Operation of Radar

Basically radar is composed of a transmitter, a receiver, a duplexer and an antenna (Figure-2.1). This configuration is called monostatic radar since transmitted and reflected waves use the same antenna. Power is transmitted through the duplexer to antenna in the form of electromagnetic wave with periodic pulses. The waves travel in free space and if there is an object, the incident waves are absorbed by that object. Then the object reradiates the waves around. A part of this reradiated wave returns back to antenna (reflected wave). Reflected wave at the antenna is directed to receiver by the duplexer. Hence a signal is sensed at the receiver by the presence of the object at a delay of τ after pulse transmission (Figure-2.2). The delay τ is related to range with the speed of radio waves which is a form of light. Speed of light is denoted by c and in free space it is equal to $3x10^8$m/s.
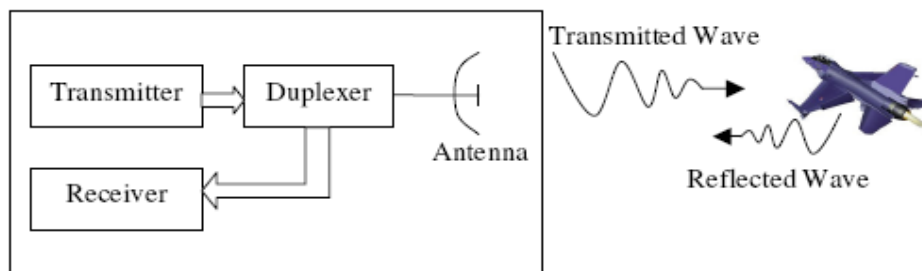
Figure-2.1 Simple monostatic radar configuration [10].

Transmitted
Waveform

Received
Waveform

τ

τ
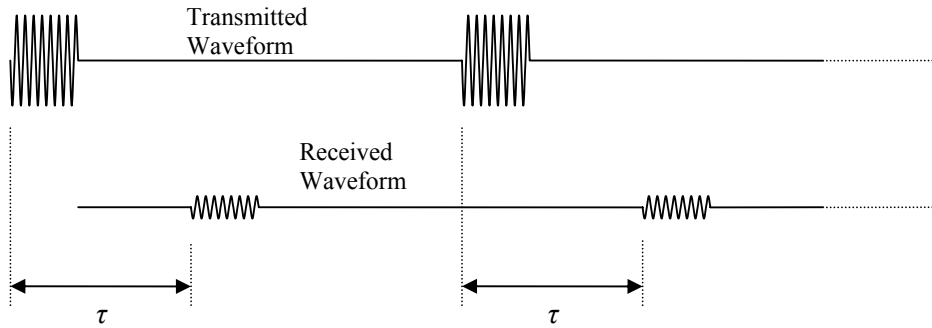
Figure-2.2 Signal waveforms in pulse modulated radar. The delay τ and received power are related to range of object.

Radio waves travel to object over R distance and backscatter to radar again over R distance with the speed c. Hence the distance R is given by the equation:

$$R = \frac{c \times \tau}{2} \tag{2.1}$$

With (2.1), range of an object is related to the time delay in free space. But since the electromagnetic waves are transmitted with periodic pulses, ambiguities may occur if the delay is larger than the pulse period.

Besides pulse modulation, there are many different techniques such as pulse compression, pulsed Doppler or continuous wave those have their own advantages.

2.1.2   Basic Radar Equation

Basic radar equation relates the received power from an object to radar parameters, range and object properties.

Assume that the object is at a distance R from the transmitter antenna. If the power transmitted by an isotropic antenna (an antenna which radiates in all directions uniformly) is denoted by P_t and the surface area of a sphere centered at antenna radius R is $4\pi R^2$ then the power density Φ_i on the surface area is:

$$\Phi_i = \frac{P_t}{4\pi R^2} \tag{2.2}$$

Generally, radar is equipped with directive antennas to observe a certain direction. Hence using a transmitting antenna gain G_t with (2.2) Φ_d is obtained as:

$$\Phi_d = \frac{P_t G_t}{4\pi R^2} \tag{2.3}$$

The object absorbs a part of incident power and reradiates it in all directions. A portion of incident power is reflected back to the antenna. Radar cross section σ is defined as the ratio of reradiated power P_a in the direction of incidence to the intercepted power density Φ_d.

$$\sigma = \frac{P_a}{\Phi_d} \tag{2.4}$$

Power density Φ_r of the reflected wave is:

$$\Phi_r = \frac{P_a}{4\pi R^2} \tag{2.5}$$

If A_e is defined as the effective area of antenna, from (2.3), (2.4) and (2.5) received power is:

$$P_r = \frac{P_t G_t A_e \sigma}{(4\pi)^2 R^4} \tag{2.6}$$

From antenna theory, G_r is related to A_e as:

$$G_r = \frac{4\pi A_e}{\lambda^2} \tag{2.7}$$

Finally, basic radar equation is combined from (2.6) and (2.7) as:

$$P_r = \frac{P_t G_t G_r \lambda^2 \sigma}{(4\pi)^3 R^4} \qquad (2.8)$$

As M. I. Skolnik [1] stated, (2.8) must be inspected carefully. Equation is valid if the gain is constant as a function of the wavelength. This fundamental equation also gives an idea about the relation between range and signal power. However there are many other factors and errors which affect the received power and signal properties. Some of them will be inspected throughout the thesis.

2.2 FM-CW Radar Background [1], [7], [11]

2.2.1 Operation of FM-CW Radar

FM-CW radar operates with continuous wave (CW) instead of pulse modulation. FM-CW is a subclass of CW radars. But in addition to CW (which has only speed detection) it has range detection capability.

Doppler effect is a well known fact that if the observer and source of oscillation is in motion with respect to each other, a shift occurs in the frequency. Assume the wavelength of transmitted wave is λ and the range from radar to object is R, then the total phase difference ϕ between the transmitted and the received waves is given by $4\pi R / \lambda$. In the case of relative motion, R and ϕ change with time. This change is expressed with angular frequency as follows:

$$w_d = \frac{d\phi}{dt} = \frac{4\pi}{\lambda} \frac{dR}{dt} = \frac{4\pi V_r}{\lambda} \qquad (2.9)$$

where V_r is the radial velocity of object with respect to radar. If f_o is the frequency of oscillation of radar then using (2.9), Doppler frequency is:

$$f_d = \frac{2V_r f_o}{c} \qquad (2.10)$$

As given in (2.10) CW radars receive a signal which is shifted in frequency by an amount of f_d in the case of relative motion. But this information is not suitable to determine range from received signal.

In FM-CW radars the transmitted signal is frequency modulated. Hence the delayed signal is received with a different frequency even if the target is stationary. The received and the transmitted waves are mixed in the radar to give a mixed signal which carries information about speed and range of the target. Figure-2.3 shows the block diagram of a simple FM-CW radar.
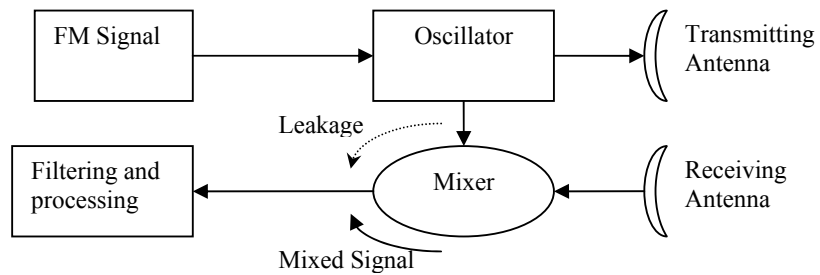
Figure-2.3 Block diagram of a simple FM-CW radar.

In general an FM modulated signal $s_t(t)$ is transmitted where θ_t(t) is phase and A is the amplitude of the transmitted wave.

$$s_t(t) = A\cos(\theta_t(t)) \qquad (2.11)$$

Due to reflection mechanism of electromagnetic waves and reflections from different ranges $s_r(t)$ is received.

9

$$s_r(t) = A_r(t-\tau)\cos(\theta_t(t-\tau)+\phi_0)$$
(2.12)

In (2.12), A_r denotes the amplitude of the received signal in relation with delay τ, in order to reflect the effect of many different scatterers from different ranges. ϕ_0 is the phase difference due to reflection. The mixed signal $s_m(t)$ is obtained from multiplication of (2.11) and (2.12) as:

$$s_m(t) = A_m(t,\tau)\cos(\phi_d(t) - \theta_t(t-\tau) - \phi_0) + A_l U_d(t)$$
(2.13)

where ϕ_d is phase and $U_d(t)$ is the amplitude of the leakage signal from the transmitter and A_l is the leakage gain.

In (2.13), the first term carries the information about the range and the relative speed of object. The second term is an unwanted signal and it is one of the major problems in range determination.

2.2.2   Parameters of Triangular Modulation for FM-CW Radar

Figure-2.4 illustrates the transmitted and the received waveforms in triangular modulated FM-CW radar where f_o denotes the center frequency of the transmitted wave, Δf denotes the deviation in frequency, f_m is the frequency of modulating signal and τ is the delay between the transmitted and the received waves.

Ideally from (2.13) neglecting the leakage and assuming the target is a point reflector, triangular FM modulation gives the following signal:

$$s_{mt}(t) = A_m \cos(\theta_t(t) - \theta_t(t-\tau))$$
(2.14)

10
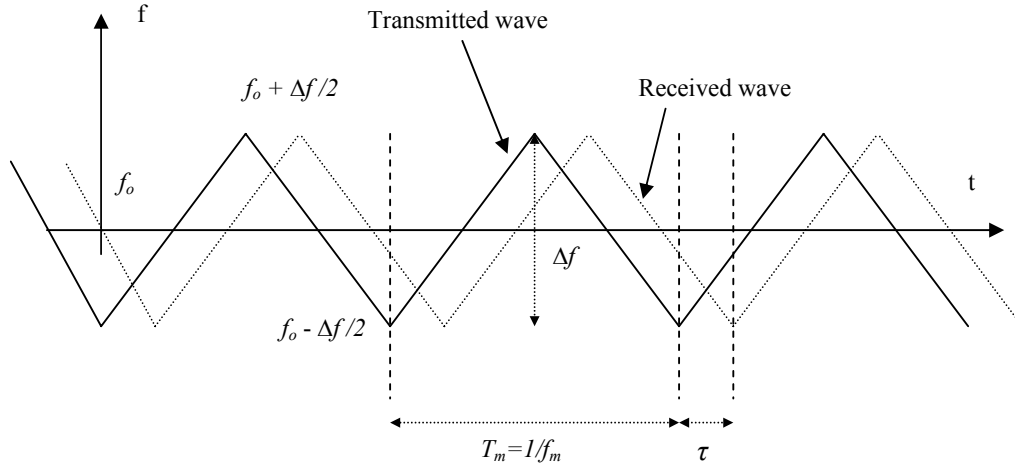
Figure-2.4 Transmitted and received waveforms in triangular modulated FM-CW radar [11].

The instantaneous frequency f_b is given by the equation:

$$f_b = f_i(t) - f_i(t - \tau) = \frac{1}{2\pi} \frac{d(\theta_t(t) - \theta_t(t - \tau))}{dt} \qquad (2.15)$$

where $f_i(t)$ is the instantaneous frequency of transmitted wave and $f_i(t\text{-}\tau)$ is the instantaneous frequency of the received wave. If the waveforms are inspected (Figure-2.4) beat frequency is constant except the turn around points of the triangle. At the rising edge of triangle the slope α of $f_i(t)$ is $2 \cdot \Delta f \cdot f_m$.

Hence, using the definitions above:

$$f_b = f_i(t) - f_i(t - \tau) = \alpha \cdot \tau = \frac{4\Delta f \cdot R \cdot f_m}{c} \qquad (2.16)$$

If K is defined as range sensitivity constant then beat frequency is:

$$f_b = K \cdot R \tag{2.17}$$

Equation (2.16) relates f_b to R with design parameters except turn around point. Beat frequency versus time is given in Figure-2.5. If the target is moving towards the radar then f_b is shifted by the Doppler frequency f_d (Figure-2.6).
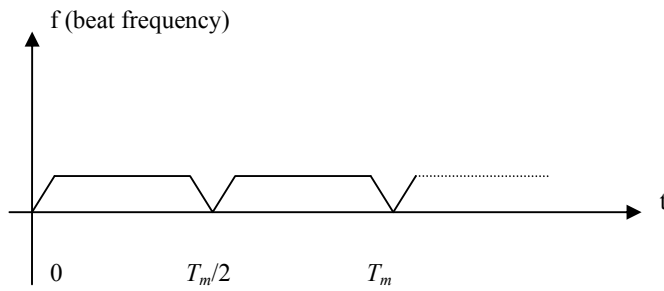
Figure-2.5 Beat frequency for triangular modulation and stationary target.
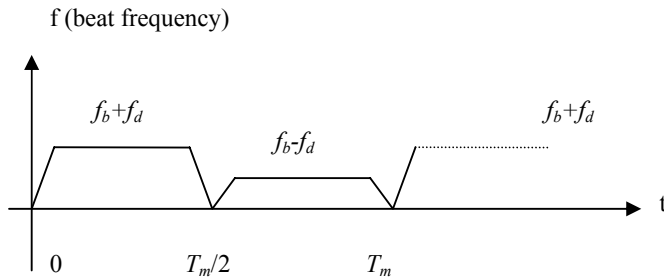
Figure-2.6 Beat frequency for triangular modulation and approaching target.

2.3 Radar Cross Section (RCS) [1], [12], [13]

RCS is a measure of radar signal reflectivity of target. In other words RCS is the area of target seen by the radar as if the target radiates equally in all directions. The formal definition is given as follows:

$$\sigma = \lim_{R \to \infty} 4\pi R^2 \left[\frac{E_r}{E_i} \right]^2 \qquad (2.18)$$

where R is the distance between the radar and the target, E_r is the reflected field strength at radar and E_i is the incident field strength at target.

However many man-made objects and natural targets are too complex to be explained simply with above equation. Neverthless RCS of objects are strictly related with wavelength of radar, grazing angle of radar waves (depression angle) and size of objects.

Skolnik [1] presents a summary of RCS for different targets (Table-2.1).

Table-2.1 General summary of RCS of targets.

Type of Target	Aspects	Cross Section, m^2
Small jet fighter aircraft or small commercial jet	Nose, tail ,	0.2-10
	Broadside	5-300
Medium bomber or midsize airline jet	Nose, tail	4-100
	Broadside	200-800
Large bomber or large airline jet	Nose, tail	10-500
	Broadside	300-550
Wooden minesweeper, 144 m long, from airborne Radar (5-10 GHz)	Broadside	10-300
	25^0 from bow, stern	0.1-300
Small bird(450 MHz)	Average overall	$10^{-5.6}$
Large bird(9 GHz)	Broadside	10^{-2}
Insect(bee) (9 GHz)	Average	$10^{-2.8}$

Also the polarization of radar and geometry of target is very important for RCS. Polarization of an electromagnetic field describes the orientation of electric field at a given point in space during one period of oscillation [12]. The re-radiation of a target is strictly related with the type of polarization. If a target is illuminated with one type of polarization it re-radiates and only carries information about that type of polarization related to its geometry. For example if a thin horizontal rod is illuminated with horizontal polarization it re-radiates, carrying information about the height of rod. However if the same rod is illuminated with perpendicular polarization, then only the thin area is intercepted by the waves and a small portion of power is re-radiated which means very low RCS value. For detailed theory of polarization refer to [12].

For the case of FM-CW radar, altitude over a large surface is considered. Hence the RCS of land and sea is inspected in more detail in the following sections.

2.3.1   RCS of Land and Sea

As Blake [13] states, a large surface (such as land surface) consist of distributed targets composed of statistically uniform assemblage of scatterers with random distribution of size and spacing. Since the land is composed of many random scatterers, the resultant signal at the receiver is the vector-phasor sum of fields from each individual scatterer. To illustrate, assume there are n equal scatterers (σ_1) whose phases are randomly distributed over 2π (incoherent wave). The expected value of σ is given by:

$$\overline{\sigma} = \sum_{i=1}^{n} \sigma_i = n\sigma_1 \qquad (2.19)$$

In the case of coherent wave the reflected waves are all in the same phase and the expected value of σ is given by:

14

$$\bar{\sigma} = \sum_{i=1}^{n} \sqrt{\sigma_i} = n^2 \sigma_1 \qquad (2.20)$$

In general, a rough surface is composed of coherent scatterers and incoherent scatterers. If the surface is very rough it is composed of only incoherent scatterers.

Normalized RCS is another definition, introduced by H. Goldstein for land and sea. It relates the illuminated area A of radar to RCS as:

$$\sigma = \sigma^o A \qquad (2.21)$$

This definition is commonly used to describe reflectivity properties of land and sea as a function grazing angle.

R.E.Clapp, depending on his experiments, related grazing angle θ to normalized RCS. According to Clapp, surface is divided in many layers of spheres and each sphere absorbs and reradiates 1-δ portion of power, where $\delta = \gamma$ is a constant related with the surface. Including near vertical angles normalized RCS can be expressed as:

$$\sigma^o(\theta) = \delta \sin(\theta) + A.e^{-B \cdot (90-\theta)} \qquad (2.22)$$

where A and B are related with surface roughness and their average values are 10 and 0.2 respectively [12]. As the surface roughness increases, A and B decreases and increases respectively [12]. Some of the δ are 10^{-4} for sea state-3 and roads, 10^{-3} for sea state-5, between 10^{-2} and 10^{1} for grass, $10^{-1.5}$ for trees and 1 for urban area and mountains [12].

(2.22) is agreed with many experiment results. General dependency of σ^o on θ for different frequencies is given in Figure-2.7.
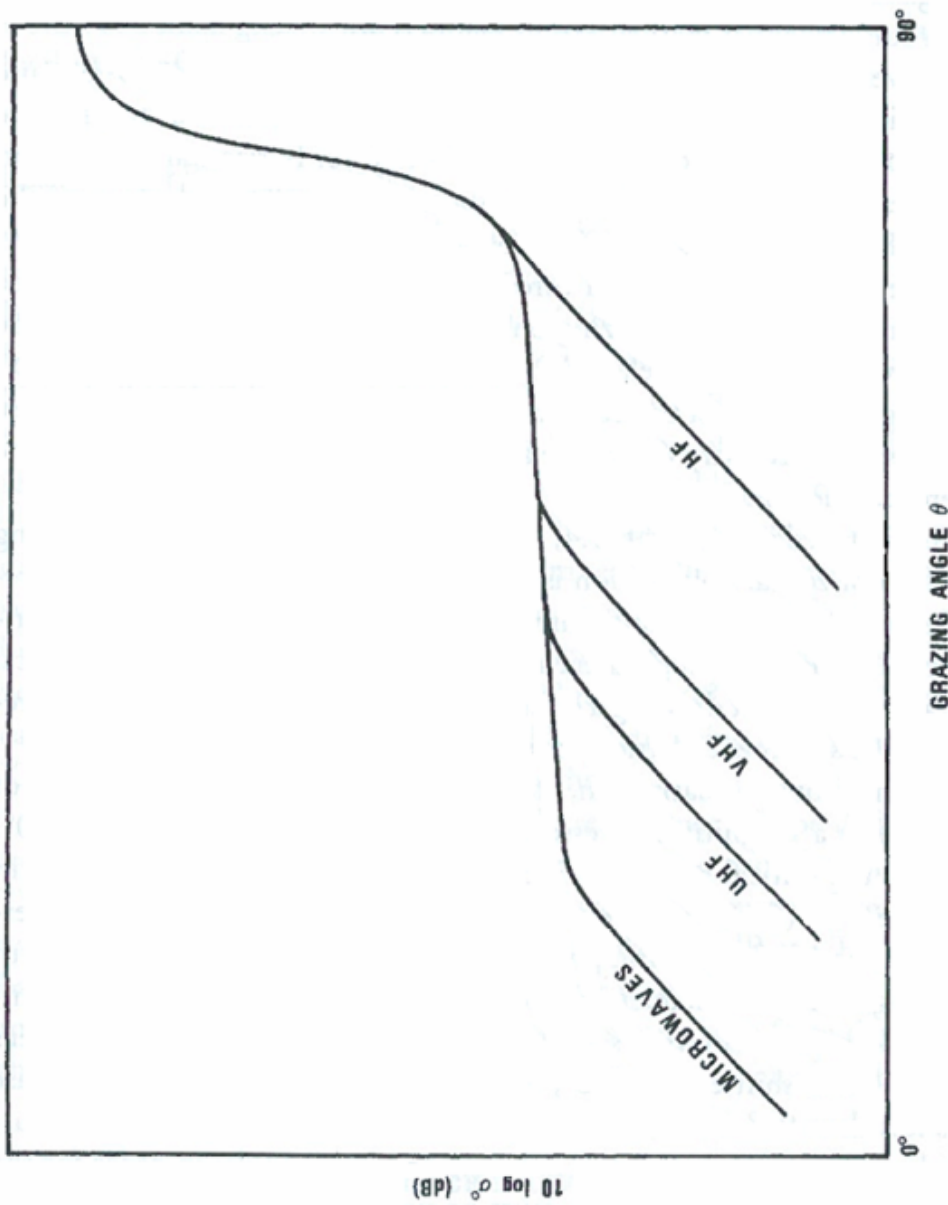
Figure-2.7 General dependence of σ^o on grazing angle θ.

16

Another factor affecting RCS is fluctuation due to wind or other factors. Sea is composed of many randomly moving scatterers and rapid fluctuations and in general many of the sea echoes are approximated by Rayleigh probability density function.

$$P(r) = \frac{r}{b^2} e^{\frac{-r^2}{2b^2}}$$
(2.23)

According to Long [12], Rayleigh approximation is probably never valid over the total power range of density function. Sea echo is intermediate between lognormal and Rayleigh distributions.

Land echo can be modeled as a combination of random scatterers or random scatterers and a constant scatterer. This can be represented by Rayleigh distribution plus a constant (Lognormal distribution and Ricean distribution). According to D. K. Barton [15], at low grazing angles RCS fluctuation is of the type Weibull ((2.24) is the probability distribution of Weibull distribution) and lognormal, in which the tails of pdf decays more slowly causing seldom spikes over the average.

$$f(x) = a \cdot b \cdot x^{b-1} \cdot e^{-ax^b}$$
(2.24)

Figure-2.8 describes the RCS fluctuation probability density of land with wind. Figure-2.9-2.11 reflect the RCS of land and sea as a function of grazing angle.
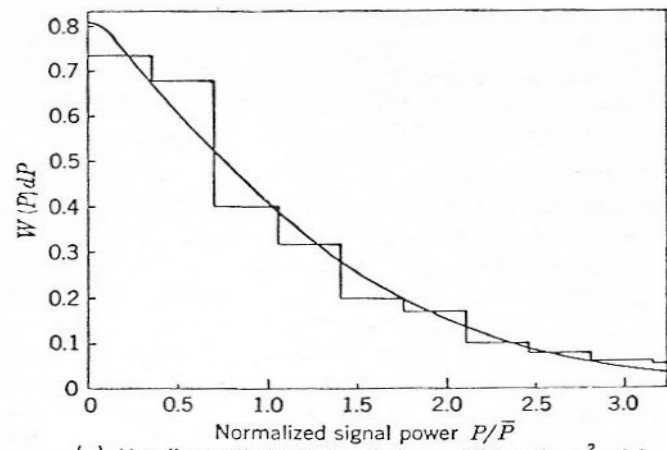
(a) Heavily wooded terrain, wind speed 25 mph, $m^2 = 0.8$
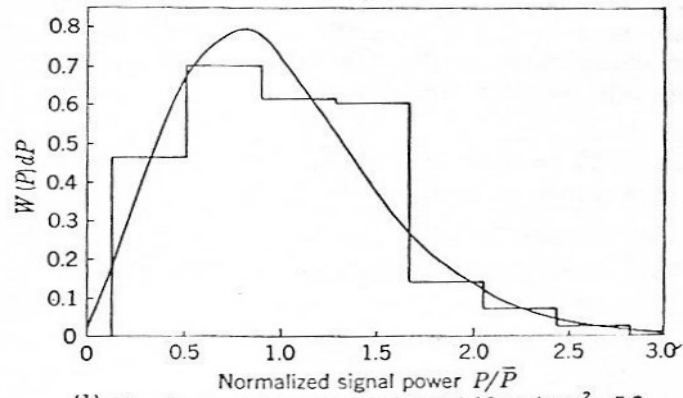
(b) Heavily wooded terrain, wind speed 10 mph, $m^2 = 5.2$
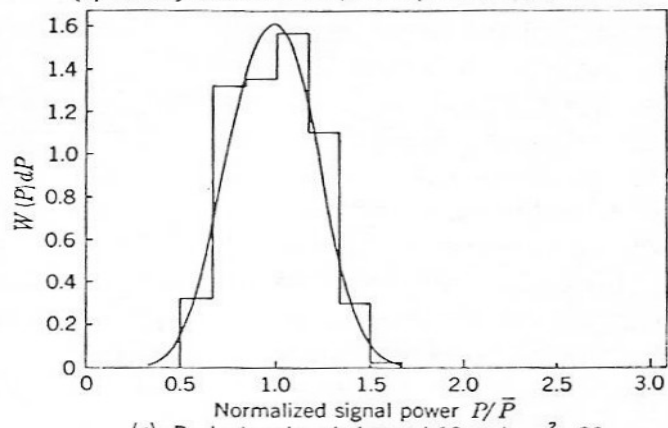
(c) Rocky terrain, wind speed 10 mph, $m^2 = 30$

Figure-2.8 RCS pdf's for land with wind [12].
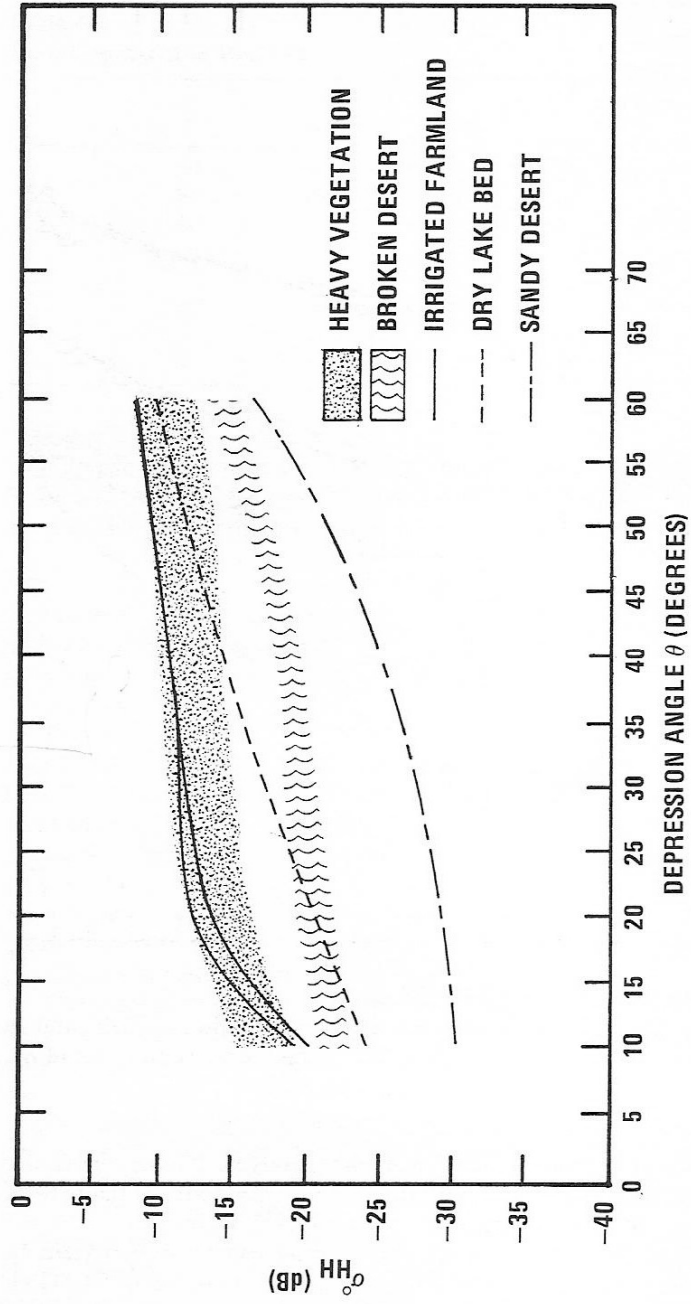
Figure 2-9 $\sigma^o{}_{hh}$ for various terrain types at X band [12].

19
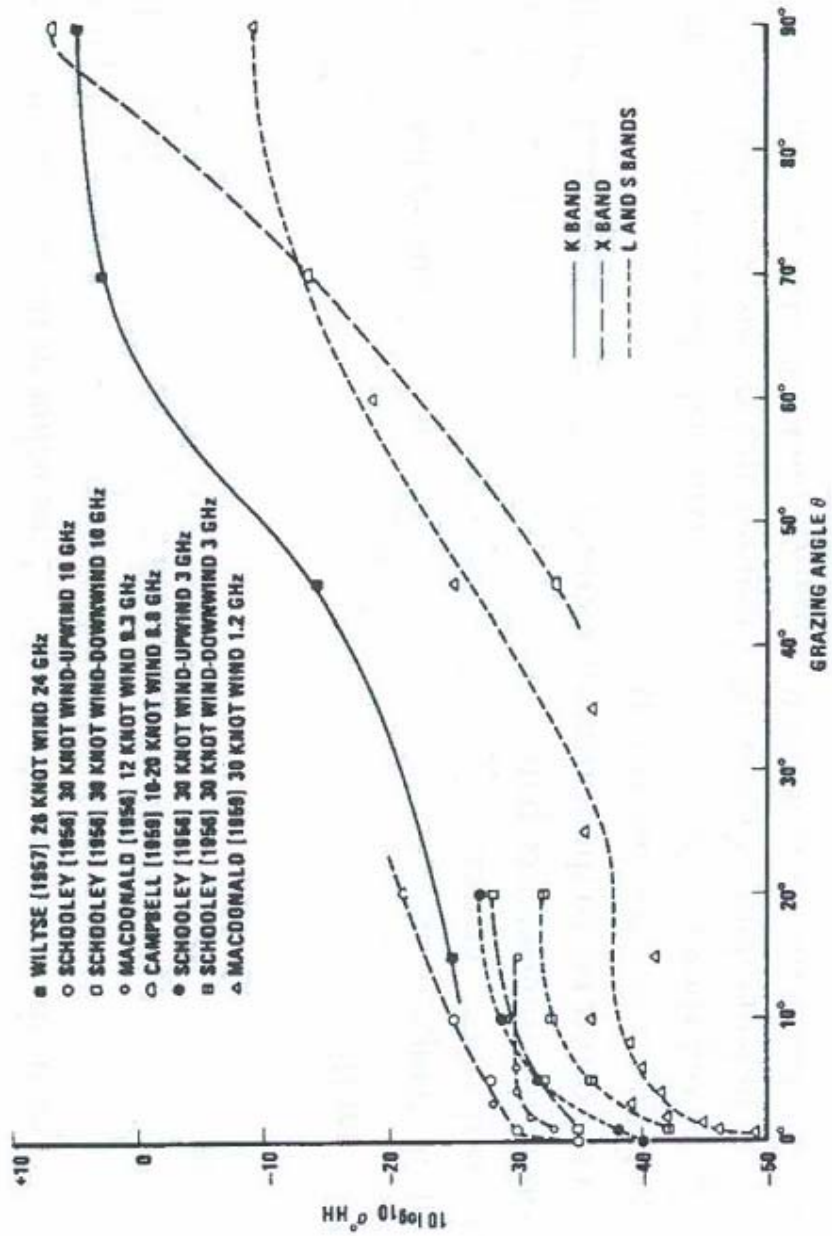
Figure 2-10 Measured values of σ^o for sea at different frequencies [12].

20
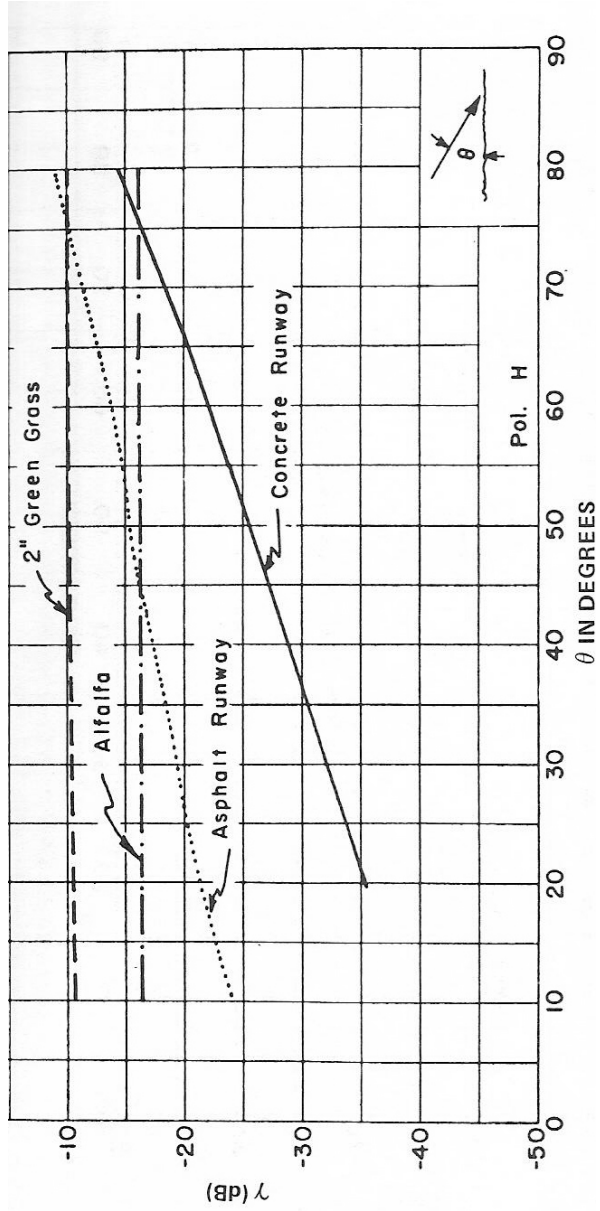
Figure-2.11 Grazing angle θ dependence of various terrains at K band [12].

2.4   Average Impulse Response of Rough Surfaces [14]

As G. S. Brown points [14], rough surface power return can be expressed as a function of delay time. This is achieved with convolution of transmitted power over a quantity involving σ^o, height h and beam width of antenna.
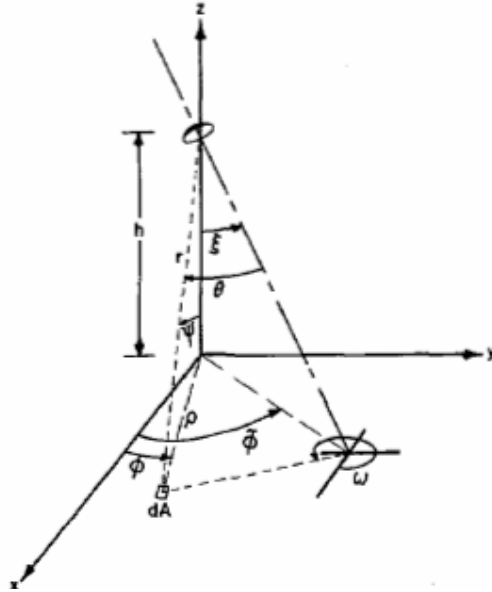
Fig-2.12 Geometry for flat surface impulse response [14].

The boresight axis of the antenna makes an angle ξ with respect to the *z* axis and an angle **Φ** with respect to the **x** axis. The angle **θ** is measured from the antenna boresight axis to the line from the antenna to the elemental scattering area *dA,* while **Ψ** is the angle this line makes with respect to the *z* axis. The antenna is at a height **h** above the *x-y* plane.

G. S Brown summarizes the necessary conditions for (2.25) to be valid. Resultant average power return versus time delay can be calculated as follows, where L_p is the two way return loss, $G\ (\theta,\ \omega)$ is the antenna gain and *r* is the range from the antenna to area dA.

$$P_{fs}(t) = \frac{\lambda^2}{(4\pi)^3 L_p} \int\limits_{illumunated\_area} \frac{\delta(t-t_r)G^2(\theta,\omega)\sigma^o(\psi,\phi)}{r^4}dA \qquad (2.25)$$

However this kind of approach has limited use since surface statistical properties must be homogenous. Also rapid fluctuations or fading nature of response must be added to average return.

Matlab calculation results are given in Chapter 3, based on average power return of random scatterers from different types of rough surfaces. However a better channel model is required, carrying information about the statistical properties to reflect the fluctuating nature of power spectrum and triangular FM-CW modulation.

2.5   Channel Model

Due to many independent scatterers received signal is random and have fluctuating nature. In order to model the surface reflection and received power, channel model must be included. As discussed in previous sections most general and analytically traceable results can be obtained with Rayleigh voltage distribution.

In fact sea can be modeled with Rayleigh distribution down to critical grazing angles (down to 10-20°). Also land clutter can be modeled with Rayleigh distribution around near-vertical grazing angles [15]. At lower angles it is usually modeled with Weibull and lognormal distributions.

In the simulation of sea and land clutter Rayleigh and Weibull distributions are used for simplicity and analytical tractability.

2.6   Processing and Detection [11], [15]

Simply two approaches can be used for signal processing of FM-CW Altimeter. Analog signal processing and digital signal processing (DSP). In analog signal processing a bank of filters are placed in parallel. Frequency responses of the parallel

filters are window shaped and center frequencies are consecutive. The outputs of the filters are followed by a threshold detector. As soon as the output of selected filters exceeds the threshold, it is understood that beat frequency is around the center frequency of that filter hence the desired range is detected.

However, real life is not that simple. The results are very coarse and erroneous due to reliability of components and fluctuating nature of radar reflectivity.

DSP is the other (preferred) approach for height detection in FM-CW radar altimeter. Straightforward way of processing the received signal is as follows. After band pass filtering the received signal to eliminate unwanted and parasitic signals and noise that is out of band, sample the signal with an appropriate rate, pre-process and apply fast Fourier transform (FFT) to get power spectrum. Next determine the threshold level according to signal and noise levels. Finally determine whether the desired frequency (hence the desired range) components exceed the threshold.

2.6.1   Sampling and FFT Parameters

DSP starts with sampling. Referring to (2.17) maximum beat frequency is given by:

$$f_{b\max} = K \cdot R_{\max} \tag{2.27}$$

According to sampling theorem to avoid aliasing a signal must be sampled at least at a double rate of maximum frequency content. Hence the sampling frequency f_s is given as:

$$f_s > 2 f_{b\max} \tag{2.28}$$

$$f_s > 8 \frac{\Delta f \cdot R_{\max} \cdot f_m}{c} \tag{2.29}$$

After determination of the sampling parameters for range, resolution is determined using N point real FFT. But before FFT, pre-processing of raw data might be necessary. Hence the data is grouped and filtered by a window to eliminate the frequency spread of spectrum. This spread is caused by the turn around points of triangular modulation. Parameter Δf_x defines frequency resolution of discrete spectrum. If Doppler shift is included (Figure-2.6) beat frequencies must be separately calculated. Since the FFT will be calculated with N points in $T_m/2$ period:

$$f_s = \Delta f_x \cdot N \tag{2.30}$$

$$\Delta f_x = \frac{f_s}{N} = 2f_m \tag{2.31}$$

Resolution of the power spectrum can be adjusted with f_s and N. From Δf_x and range sensitivity K, range resolution ΔR can be calculated as:

$$\Delta R = \Delta f_x / K = 2f_m / \frac{4\Delta f \cdot f_m}{c} = \frac{c}{2\Delta f} \tag{2.32}$$

2.6.2   Threshold Determination

In order to avoid high false alarms rates caused by noise and interference, signal threshold must be adjusted adaptively (Constant False Alarm Rate (CFAR) calculation). Noise is assumed to be additive white Gaussian (AWG) and $\gamma.k$ is the threshold in power spectrum where k is a constant. In (2.33), γ is the average power of noise signal in one period and calculated from signal power spectrum of noise only. If the normalized signal power exceeds threshold $\gamma.k$, height can be determined.

$$P_{avg} = \frac{1}{N} \sum_{n=<N>} |x_n|^2 = \gamma = \sum_{k=<N>} |a_k|^2 \tag{2.33}$$

2.6.3   Effect of RCS Fluctuations

As Barton [15] states most of the land clutter fluctuations have spreads described by lognormal and Weibull distributions. Although CFARing works well with Rayleigh type distributions, lognormal and Weibull distributions cause random spikes. This nature of land clutter generates excessive false alarms. This kind of false alarm rates can be handled with order statistics. By order statistics the FFT results (detected frequencies) are sorted and updated with a sliding window. By a proper selection (median or between median and maximum) of measured values, the seldom spikes are avoided without loosing the range information.

CHAPTER 3

CALCULATIONS AND SIMULATIONS

3.1 Overview of Trimod6 Simulator

To compare the measured height with the real height and evaluate the performance of the FM-CW radar altimeter, a simulator is generated in Matlab called Trimod6 simulator. This simulator is mainly composed of two parts. First part is a core simulator which calculates the impulse response for different sea and terrain types. With this response, simulator obtains the expected output signal of the radio frequency (RF) part of FM-CW radar altimeter. Second part is a processor simulator which simulates the DSP unit of the system. Finally these two parts are combined together with the altitude determining algorithm to find range and to compare the measured heights with the heights entered into the simulator. Matlab code of Trimod6 simulator is given in Appendix D.

3.1.1 Core Simulator

This part of the simulator computes the radar echo and simulates the FM-CW radar altimeter circuits.

Firstly, a power versus range profile P_d is calculated from (3.1) in Matlab.

$$P_d(r_t) = \frac{P_c \cdot G^2(\theta) \cdot \sigma(\theta) \cdot 2\pi \cdot r}{(4\pi)^3 \cdot r_t^4} \tag{3.1}$$

where P_c denotes the power level, $G(\theta)$ denotes the antenna gain, $\sigma(\theta)$ denotes the RCS as a function of grazing angle θ in radians, r denotes the radius of each

concentric circle (Figure-3.1) and r_t denotes the range to each circle. Equation (3.1) is obtained from manipulation of (2.25) and delay is converted to range.
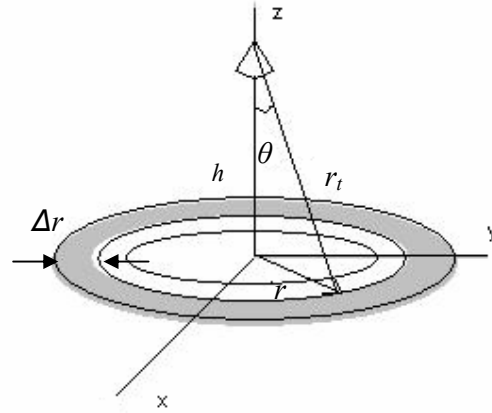
Figure-3.1 Geometry used in Trimod6 for power versus range profile.

Two of the inputs entered for the P_d are altitude h and antenna beam width θ_m. From h and θ_m maximum range is calculated. Vector r_t is calculated as discrete points between h and maximum range. The distance between each point is *step* (a parameter entered for the resolution of surface) meters. Using r_t and h, r and corresponding θ is also obtained as a vector in Matlab. $G(\theta)$ is assumed to be constant within beam width and zero outside the 3 dB beam width (Appendix B).

There are three input parameter for $\sigma(\theta)$, to simulate the reflection properties of the surface as a function of grazing angle:

$$\sigma(\theta) = rcs\_prm1 \cdot \sin(\theta) + rcs\_prm2 \cdot e^{-rcs\_prm3 \cdot (90 - 180 \cdot \theta / \pi)} \qquad (3.2)$$

Referring to (2.22) δ is denoted by *rcs_prm1*, A is denoted by *rcs_prm2*, and B is denoted by *rcs_prm3*. Also $\sigma(\theta)$ data can be entered via an excel worksheet for more sophisticated curves. For Figure-3.2 and Figure-3.3 $\sigma(\theta)$ data is entered via an excel file referring to Figure-2.11 (Appendix E) to get P_d. h is entered as 300m and θ_m is entered as 80^0. Transmitted power P_c is 1 W.

28
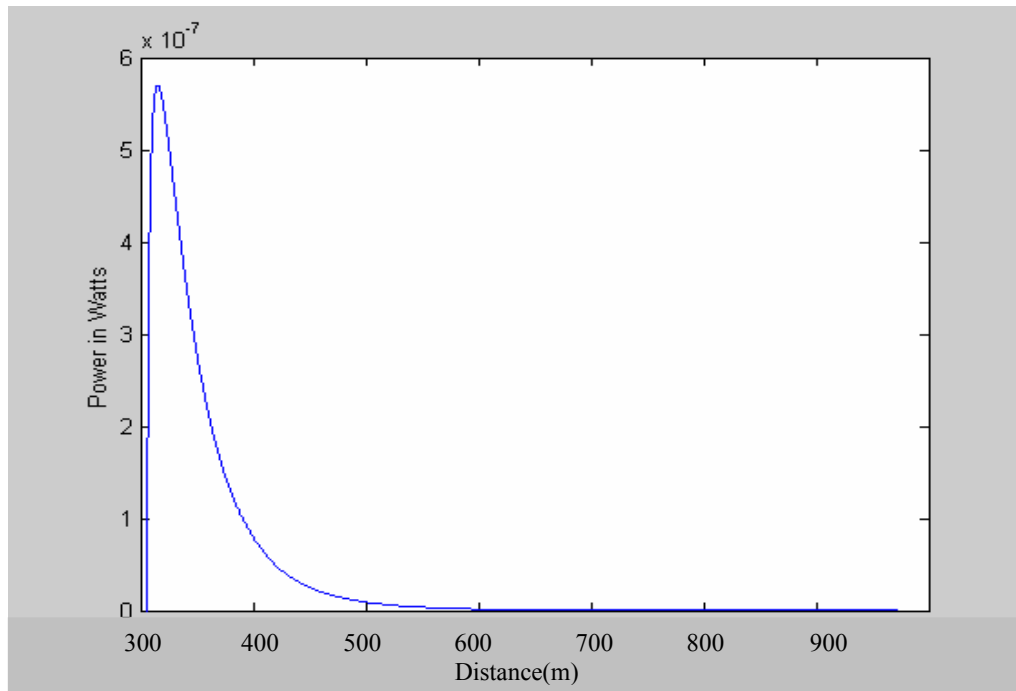
Figure-3.2 Return power of an asphalt road. (h=300 m, θ_m=80^0, P_c=1 W)
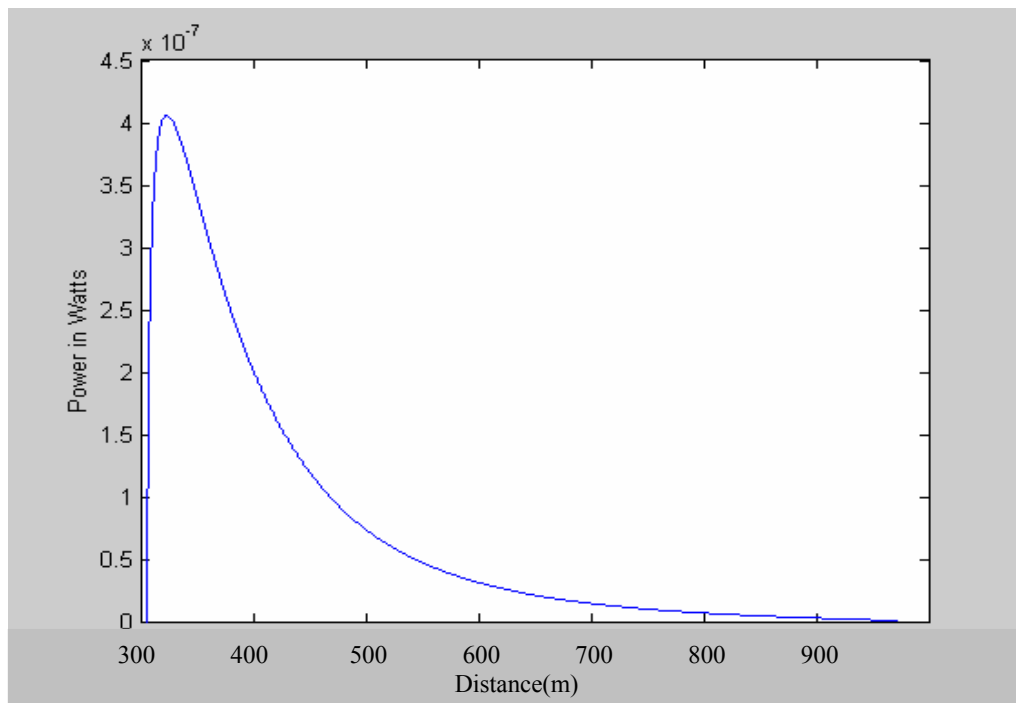
Figure-3.3 Return power of alfalfa. (h=300 m, θ_m=80^0, P_c=1 W)

Comparison of Figure-3.2 and Figure-3.3 reveals that asphalt has stronger power return near-vertical grazing angles but weaker power return at lower angles.

Secondly, the power versus range profile is fluctuated. To realize fluctuation, voltage value of each point on P_d is multiplied with a random number from Rayleigh or Weibull distributions (Figure-3.4). Each random number multiplied with the voltage value is independent by the assumption that distance between each ring is much greater than the wavelength of the transmitted wave. Rayleigh variance parameter or Weibull shape and scaling parameters must be inserted as input. Also AWGN can be inserted at any power level.

In fact by adding fluctuation to the power delay profile, impulse response $h(t)$ of surface is obtained. The impulse response is used for the simulation of FM-CW radar.
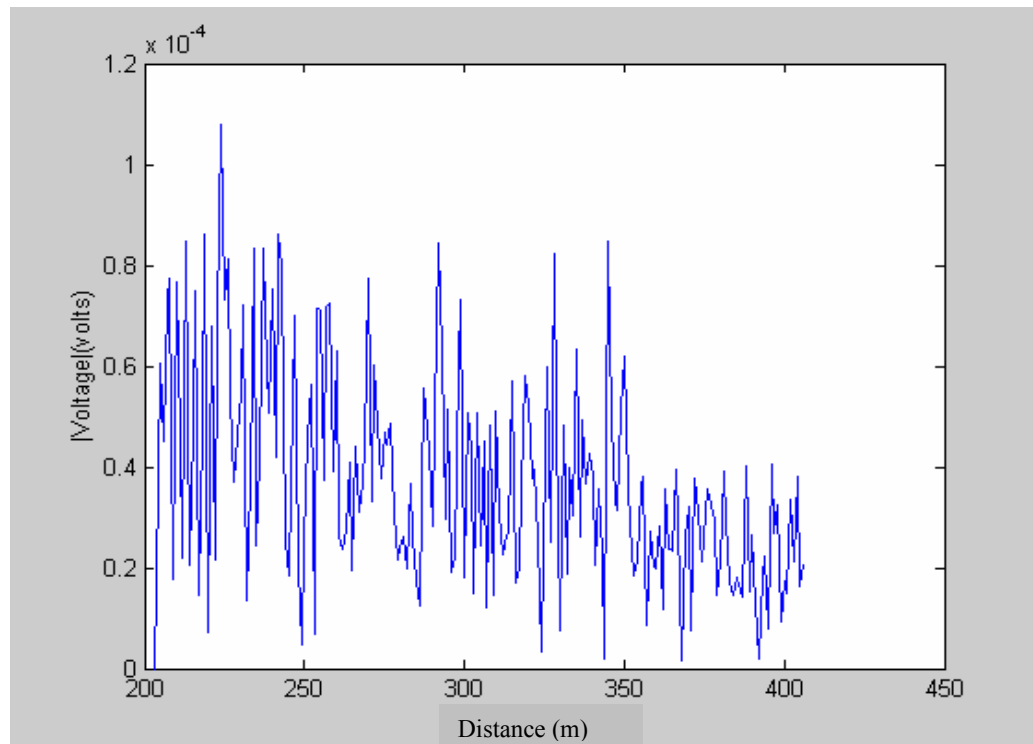
Figure-3.4 A voltage magnitude versus range profile sample for trees. (h=200 m, θ_m=60^0, P_c=1W)

Thirdly, FM-CW radar is simulated. Referring to Chapter 2 (Figure-2.4), if the transmitted signal is triangularly modulated also the received signal is triangularly modulated but it is a delayed version and additionally carries information about the surface of reflection. Referring to (2.11), let $s_t(t)$ be the transmitted wave. Then the low-pass equivalent of the transmitted signal can be expressed as:

$$s_{lt}(t) = Ae^{j\theta(t)} \tag{3.3}$$

Obviously the phase of the transmitted signal is as follows where $m(t)$ is the instantaneous frequency of the transmitted signal:

$$\theta_t(t) = k\int m(t)dt \tag{3.4}$$

On the other hand, phase of the received signal from (2.12) is:

$$\theta_r(t) = \theta_t(t - \tau) + \phi_0 \tag{3.5}$$

Figure-3.5 shows the phases of the transmitted and the received waves. ϕ_0 of the received wave is not included in Figure-3.5. Only the delay τ is included for 2000m.
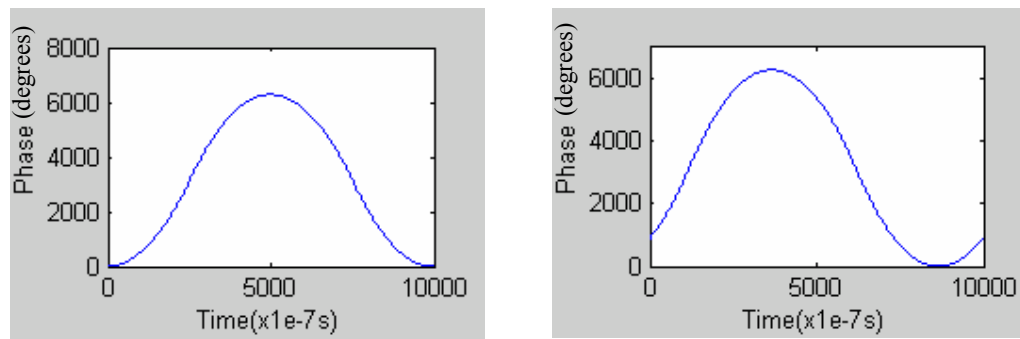
(a) Received phase (b) Transmitted phase
Figure-3.5 Phase&time graphs. (a) shows $\theta_t(t\text{-}\tau)$ and (b) shows $\theta_t(t)$ for 2000m.

Using (3.3) and (3.4) and $h(t)$, received signal $s_{lr}(t)$ and the mixed signal $s_m(t)$ are:

$$s_{lr}(t) = s_{lt}(t) * h(t) \qquad (3.6)$$

$$s_m(t) = s_{lt}(t) \cdot s_{lr}^{*}(t) \qquad (3.7)$$

where ' * ' denotes convolution and ' $(\ )^{*}$ ' complex conjugation. At this stage, noise is added and mixed signal is down sampled since it was over sampled. The reason of over sampling is high frequency content of $s_{lt}(t)$ and $s_{lr}(t)$. Additionally down sampled signal is filtered within the band of interest.

For this part of the code f_m, Δf, and sampling period can be entered as input parameters. Also filtering type and cut-off frequencies can be entered. Filtering types used in the simulator are Butterworth and Chebyshev.

3.1.2   Processor Simulator

Second main part of Trimod6 is processor simulator. This section simulates processing unit of FM-CW radar altimeter.

Output of core simulator is firstly split into two waveforms namely the rising and the falling edges of the triangle. Waveform1 belongs to rising part of the triangle and contains positive frequencies. Waveform2 belongs to falling part of the triangle and contains negative frequencies. The reason of separation is Doppler shift. Due to this shift, waveform1 and waveform2 are affected differently (Figure-2.6) but their averages are around the real height. After separation of positive and negative frequencies, waveforms are preprocessed. They are multiplied with Hamming window in order to minimize the effect of frequency spread. The spread to lower frequencies is due to turn around points of triangular modulation. Figure-3.6 shows
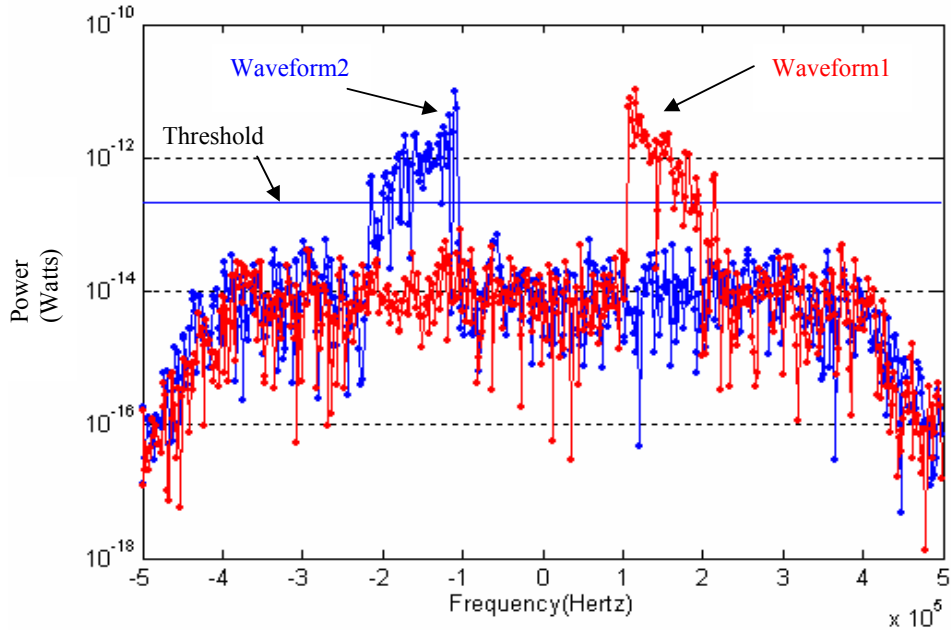
Figure-3.6: A height measurement with Hamming window. Entered parameters are h=1000m, θ_m=60^0, P_c=1W and rcs_prm1=0.1 rcs_prm2=10, and rcs_prm3=0.2 respectively. Noise power is -80 dBm.
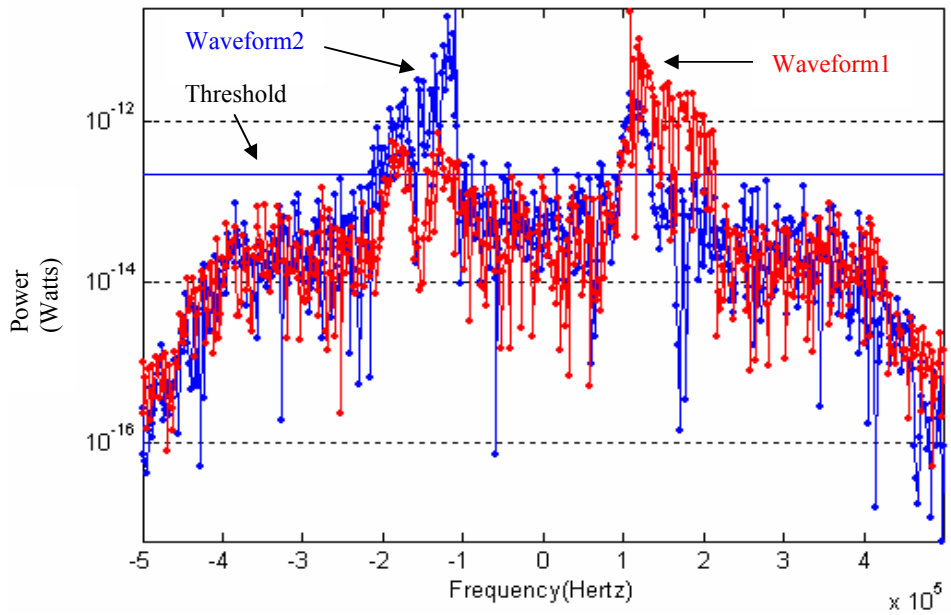

Figure-3.7: Another height measurement without Hamming window. Entered parameters are h=1000m, θ_m=60^0, P_c=1W and rcs_prm1=0.1 rcs_prm2=10, and rcs_prm3=0.2 respectively. Noise power is -80 dBm.

33

one sample of spectrum of the received signal after Hamming windowing. Figure-3.7 shows another sample of spectrum of the received signal before Hamming windowing.

Comparison of Figure-3.6 and Figure-3.7 shows the requirement of preprocessing. By windowing, the spread to lower frequencies is attenuated between 3 dB-10 dB and range accuracy is improved. The blue straight line that is parallel to frequency axis is threshold.

After preprocessing, FFT is applied to waveform1 and waveform2. From FFT results normalized power spectrums of rising and falling edges of triangle is obtained. These results are compared with the threshold separately and heights for rising and falling edges are calculated. Calculated heights are averaged and the result is obtained for one period of T_m.

The input for this section is number N of FFT points. Threshold is obtained within the algorithm and automatically updated as necessary.

3.1.3 Altitude Determining Algorithm

Objective of the algorithm is to comment on the height measurements, filter out irrelevant values and automatically adjust the parameters of altitude determination. If necessary, the user should be warned about the measurements results. Reason of the warning might be 'low power' due to a high altitude which may result inaccurate measurement or 'out of detect'. Out of detect is the case in the algorithm in which no components of power spectrums crosses threshold for more than half of the window size. Selection for the size of window as half is a practical limit for accurate altitude detection where window is the collection of detection results. Also high noise or interference may corrupt the received signal. Whatever the reason is, the problem must be sensed and reported. Finally, if the altitude can be determined properly, results must be displayed.

Flowchart in Appendix C explains the flow of algorithm. Algorithm always tries to start measurement at a proper threshold. If max power is greater than a constant times threshold, then threshold is increased else kept the same. Once the algorithm gets a *good starting point* it slides the measurement window, for example gets new result into first in first out (FIFO) buffer and discards the oldest measurement. This goes on as far as the measurement results are not contradictory. If the results are not within the tolerances the user is warned. From this point on, algorithm resets and looks for an other *good starting point*. Also the algorithm is clever that it knows whether it is going up or down. It records the relative height from height measurements and by checking relative height, it adjusts the threshold accordingly.

The algorithm accepts *n* (window size) and deltaR (standard deviation limit). Results, performances and deficiencies of algorithm are inspected in the following sections.

3.2 FFT Results and Comments

As explained in simulator overview before, there are many parameters to control simulation. Assuming that the simulation is performed between 100 m to 4000 m,

1. Let θ_m be 60^0,
2. Let window size *n* be 10,
3. Let deltaR be 3 times range resolution,
4. Let N be 512,
5. Let f_m be 1 kHz,
6. Let $\Delta f/2$ be 4 MHz,
7. Then *K* is 106 Hz/m, f_{bmax} is 400 kHz, down sampling ratio is 10
8. Then range resolution is 18.75 m and deltaR is 56.25m
9. Then sampling period is 1e-7 s

FFT results of processor simulator not only show height but also reflect the properties of terrain. For example sea state-3 and roads return occupy narrowband and a sharp peak. Hence it is easier to detect true distance and adjust threshold.

Figure-3.8 shows spectrum of radar return for 1000 m which results a peak around 100 kHz. For sea state-3 *rcs_prm1* is 10^{-4} *rcs_prm2* is 10, and *rcs_prm3* is 0.2. Noise power is -80 dBm and output power is 1 W. Noise power is adjusted according to noise floor of FM-CW radar altimeter device at room temperature. Ground reflection is of Rayleigh type and unity variance. Figure-3.9 belongs to the same height, power and noise levels but for sea state-5. For sea state-5 *rcs_prm2* and *rcs_prm3* are kept the same, *rcs_prm1* is 10^{-3}. In Figure-3.8 and Figure-3.9 straight blue lines denotes the threshold.
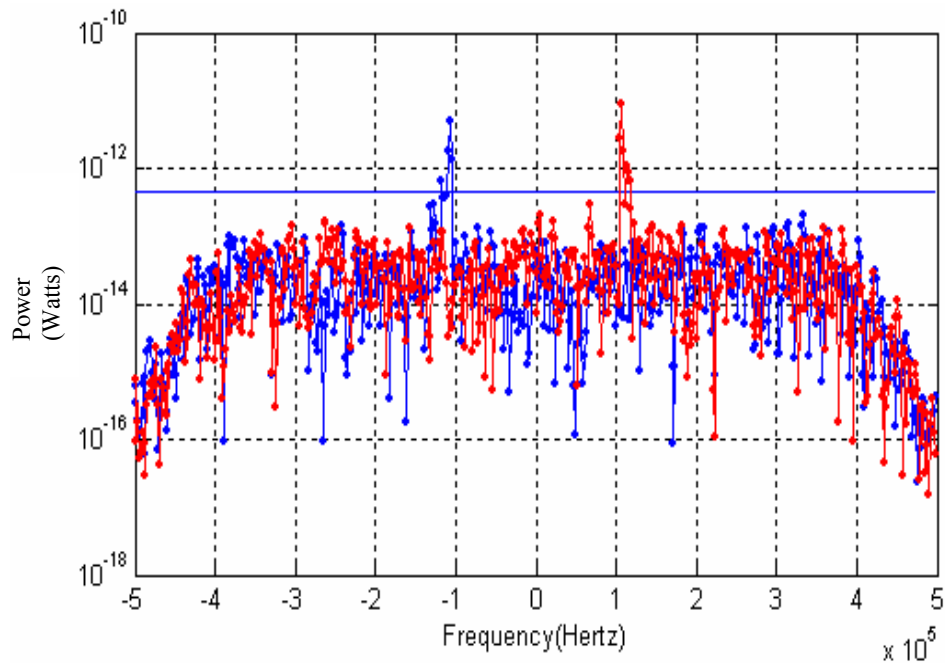
Figure-3.8: Sea state-3 and roads return. Entered parameters are h=1000m, θ_m=60^0, P_c=1W and rcs_prm1=1e-4, rcs_prm2=10, and rcs_prm3=0.2 respectively. Noise power is -80 dBm.
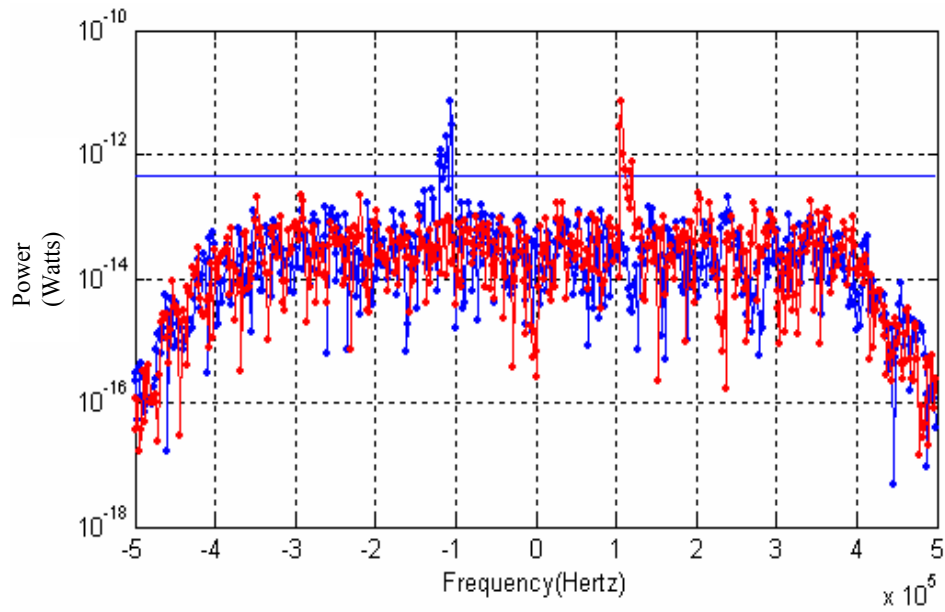
Figure-3.9: Sea state-5 return. Entered parameters are h=1000m, θ_m=60^0, P_c=1 W and rcs_prm1=1e-3, rcs_prm2=10, and rcs_prm3=0.2 respectively. Noise power is -80 dBm.
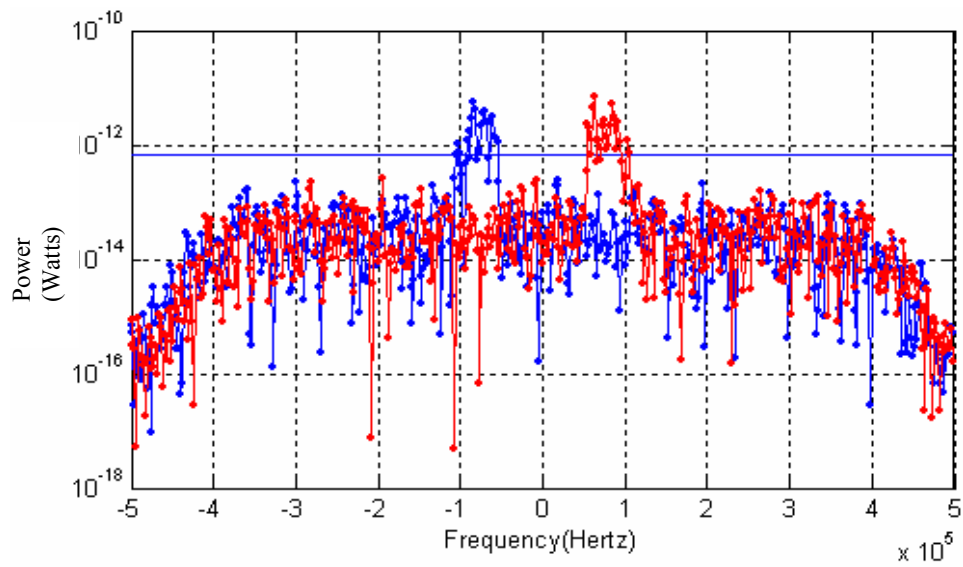
Figure-3.10: Trees return. Entered parameters are h=500m, θ_m=60^0, P_c=1 W and rcs_prm1=1e-1.5, rcs_prm2=0.1, and rcs_prm3=0.3 respectively. Noise power is -80 dBm.

Figure-3.10 simulates trees. In Figure-3.10, *rcs_prm1* is $10^{-1.5}$, *rcs_prm2* is 0.1, *rcs_prm3* is 0.3 to reflect surface roughness [12]. For the scenario in Figure-3.10 transmitted power is 1 W, noise power is -80 dBm and height is 500 m. There is less than 10 dB power difference between the rising edge at 50 kHz height and falling edge at 100 kHz. 500 m height results a peak at 50 kHz in spectrum since *K* is 106 Hz/m. Due to beam width of antenna max 1000 m of range is observed which result a falling edge at 100 kHz. For this case variance parameter of Rayleigh (vargs) is chosen as 4. More power is necessary for more accurate measurements in forest and little grazing angle dependence.
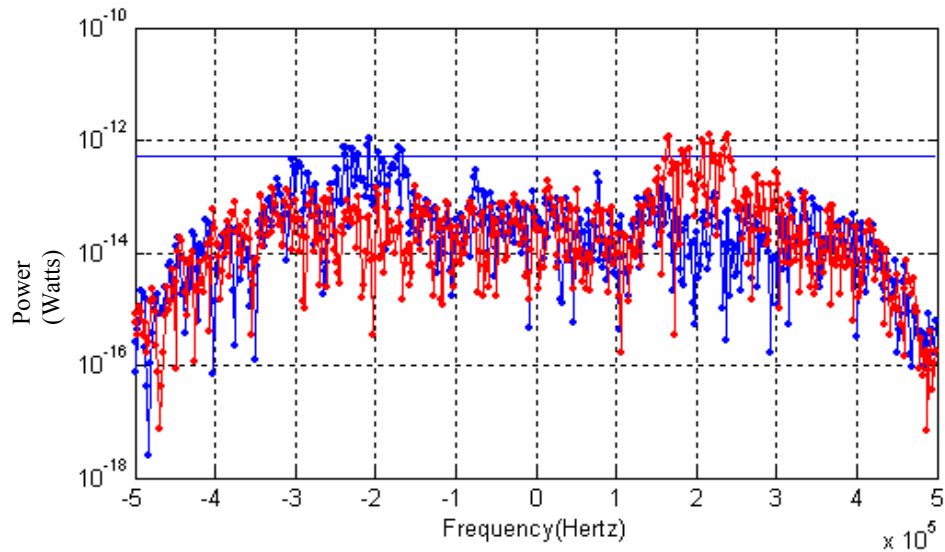
Figure-3.11: Urban area return at 1508 m. Entered parameters are h=1508m, θ_m=60^0, P_c=0.1 W and rcs_prm1=1, rcs_prm2=10, and rcs_prm3=0.2 respectively. Noise power is -80 dBm.

Another case is urban area or mountains. For this case *rcs_prm1* is 10^0, *rcs_prm2* is 10, *rcs_prm3* is 0.2. Transmitted power is 0.1 W, noise power is -80 dBm, vargs is 1. For Figure-3.11 obtained height is 1557 m where entered height is 1508 m. Radar return is more complicated and range accuracy is lower as seen in Figure-3.11. Also the low power and high noise makes the measurement less effective.

3.3 Comparison of Entered and Measured Heights, Comments on Algorithm

For the comparison of entered and measured heights, entered height into simulator is changed as if the FM-CW radar altimeter is moving up or down and outputs of the algorithm are recorded. Recorded results are plotted on the same time axis and compared. There are noise-like regions in the plot. These are the points where algorithm looks for a good starting point. These results are not displayed to user. Also there are missing points. These are no-detection samples and they are also not displayed to user. Instead if sufficient valid measurements are performed from those data, the entered height is estimated. Finally the zero spikes are the indication of *no-detection*s cases. For these cases again, algorithm looks for a good starting point.

Figure-3.12 is obtained from alfalfa RCS data as excel sheet (Appendix E) with -80 dBm noise and 10 W output power. DeltaR is set to 50. Figure-3.12 b) shows the enlarged spiky points and steps. Steps are due to the resolution of power spectrum. For this scenario output power is high enough since the results are within ± 10 m at 1900 m altitude.
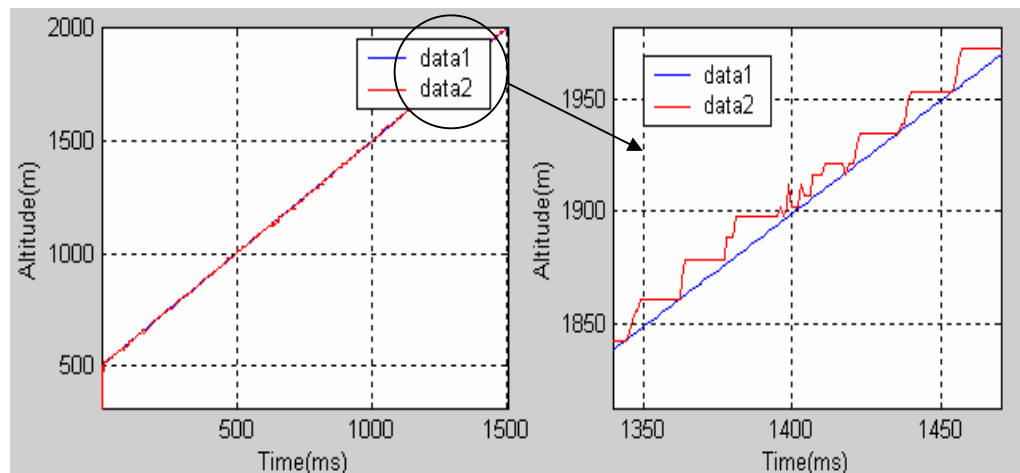
(a) altitude is between 500 and 2000 m   (b) altitude is between 1800 m and 2000 m
Figure-3.12 Comparison of entered and measured heights. Data1 stands for the entered height, data2 stands for the algorithm output. (b) is the zoomed view of (a) around 1900m.

Another scenario is for urban area or mountains. Figure-3.13 reflects the result of 500 m to 2000 m region. For urban area or mountains case, average value of *rcs_prm1* is 10^0, *rcs_prm2* is 10, *rcs_prm3* is 0.2. Output power is 0.32 W, with -80 dBm noise power. For the case in Figure-3.13 none of the FFT measurements are missed. But due to high noise and low output power (especially above 1600 m) measurements tend to vary from entered results and fluctuate greater than defined limits. Consequently, algorithm resets frequently and flows as soon as a suitable result is obtained. Above 600-700 m results tend to follow entered height with a little higher slope. The reason of higher slope is low power. In Figure-3.9 frequency content of spectrum makes a sharp peak at vertical range therefore the range is accurately detected. On the other hand frequency content of Figure-3.11 is spread to higher frequencies. So a slope adjustment can be made for low power region for more accurate measurement. Median filtering result is displayed with a warning for every *n* measurement. This is done if the measurements are valid and within standard deviation limit.

Another way used to compare the transmitted power with the height measurement accuracy is to record the random parameters. Recorded random parameters are used for all FFT measurements. Height and terrain is also kept the same but the power levels are changed and the accuracy of measurements is reflected. Table-3.1 gives an idea about the false alarms and no-detections for different power levels within a window.

Table-3.1 Transmitted power & no detections and false alarms. These results are obtained for 2000 m and sea state-5 with 1e-13 W constant threshold. Window size *n*=30.

Power (dBW)	-25	-20	-15	-10	-5	0	5	10	15	20	25
No-detection	30	30	28	15	0	0	0	0	0	0	0
False-alarm	0	0	0	0	0	0	0	0	6	25	30
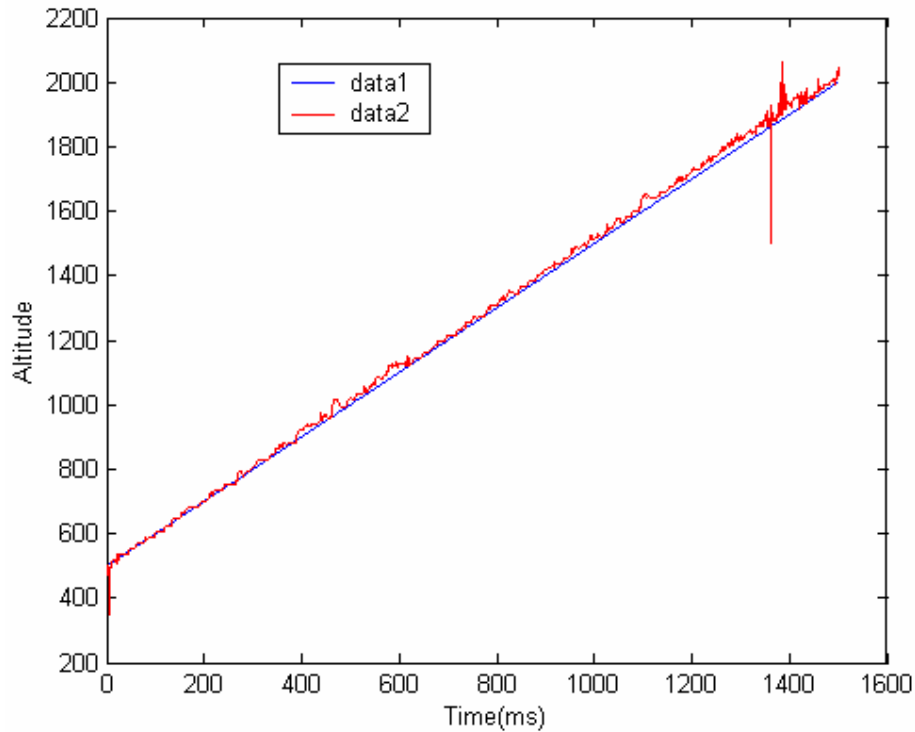
Figure-3.13 Another comparison of entered and measured heights. Data1 stands for entered heights and data2 stand for measured heights.

For Table-3.1, if the measured height is 18.75 (*resolution*) meters lower than entered height than it is accepted as false alarm. To improve the accuracy of statistics window size *n* is increased to 30. For lower altitudes in Table-3.1 power is much more than required and since the threshold is constant, false alarms occur. False alarms occur due to frequency spread. The frequency spread is caused by the crossing region of triangular modulation and even if it is attenuated by windowing high power highlights this region. On the other hand high altitudes suffer from low power and no detection.

Figure 3.14 compares the different altitude changes. Data1 belongs to constant altitude at 350 m, data2 belongs to gain altitude at 100 m/s, data3 belongs to gain altitude at 250 m/s, data4 belongs to gain altitude at 500 m/s, data5 belongs to gain altitude at 1000 m/s respectively. Black lines show actual heights. Due to resolution, mean square error is greater for the lowest slope. For the constant case the altitude

just fits the resolution step by chance. If the altitude is changed to 355 m then almost the same result is obtained (around 350 m) which means greater error.
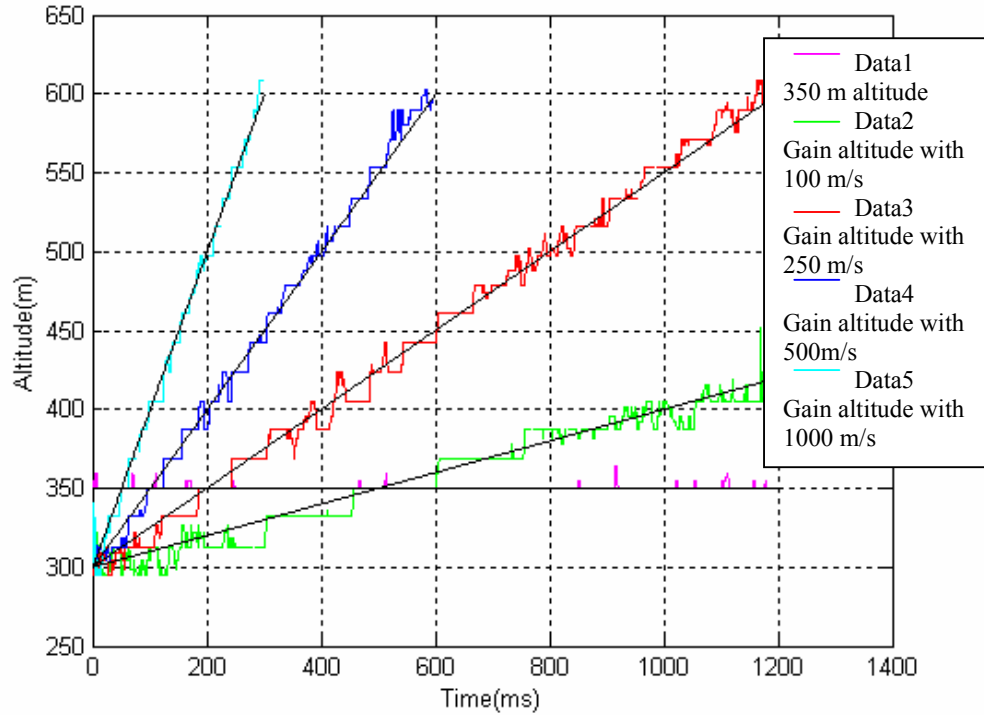
Figure-3.14 Comparison of different scenarios for altitude change.

Window size n, used for order statistics is one of the most important parameters in altitude determination. Hence it must be inspected in more detail. If the observation time is increased (window size n is increased) then signal to noise ratio (SNR) is increased and accuracy of measurements is also increased. However an improvement better than ΔR is not necessary due resolution of FM-CW radar altimeter. On the other hand, if median filtering is applied then due to relative speed of FM-CW, measurement result vary by $\Sigma R = n \cdot v \cdot f_m / 2$. ΣR should be smaller than ΔR for accurate measurements with relative speed. As a result an optimum window size n can be determined with the constraint ΔR.

Figure-3.15 shows the comparison of entered and measured heights for *rcs_prm1* is $10^{-1.5}$, *rcs_prm2* is 10, *rcs_prm3* is 0.2. Output power is 0.32 W, noise power is -80 dBm. Figure-3.15 shows the no detection numbers for Figure-3.16 where window size is 10. Hence more than 5 no detection numbers leads to out of detect. For this case power level should be increased.

Figure-3.17-3.20 shows the comparison of entered and measured heights for *rcs_prm1* is 10^{-3} (sea state-5), *rcs_prm2* is 10, and *rcs_prm3* is 0.2. Output power is 1 W and noise power is -80 dBm. In Figure-3.17 *n* is 32, in Figure-3.18 *n* is 16, in Figure-3.19 *n* is 8, and in Figure-3.20 *n* is 4. Comparison of different window sizes reveals that an optimum result can be obtained between *n*=8 and *n*=32.
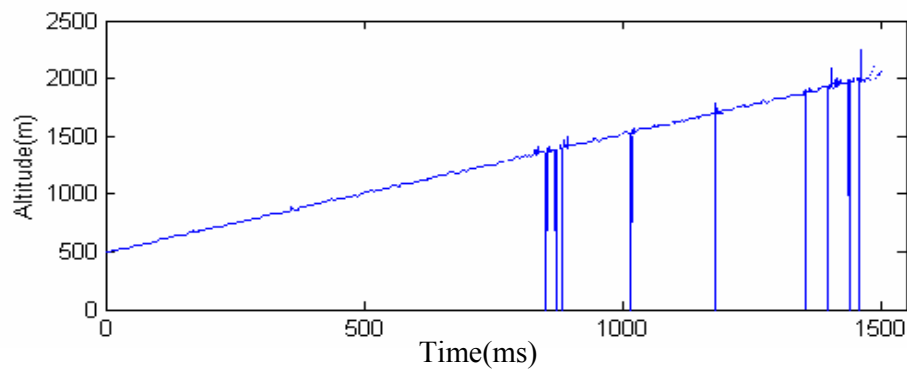
Figure-3.15 Comparison of entered and measured heights for a worse case.
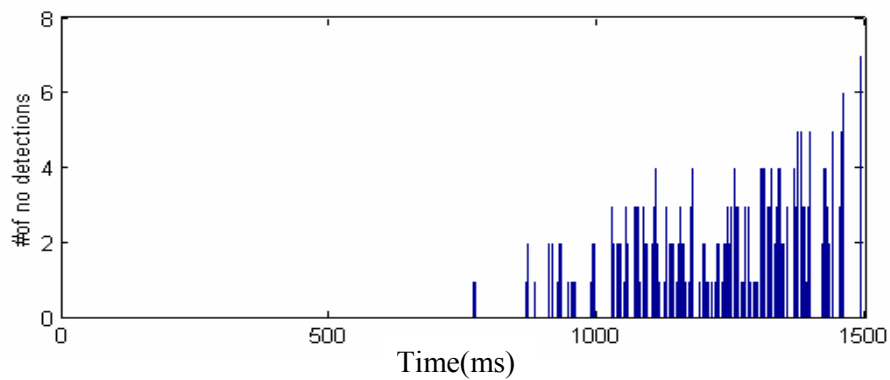
Figure-3.16 No detection numbers for Figure-3.15 with window size 10.
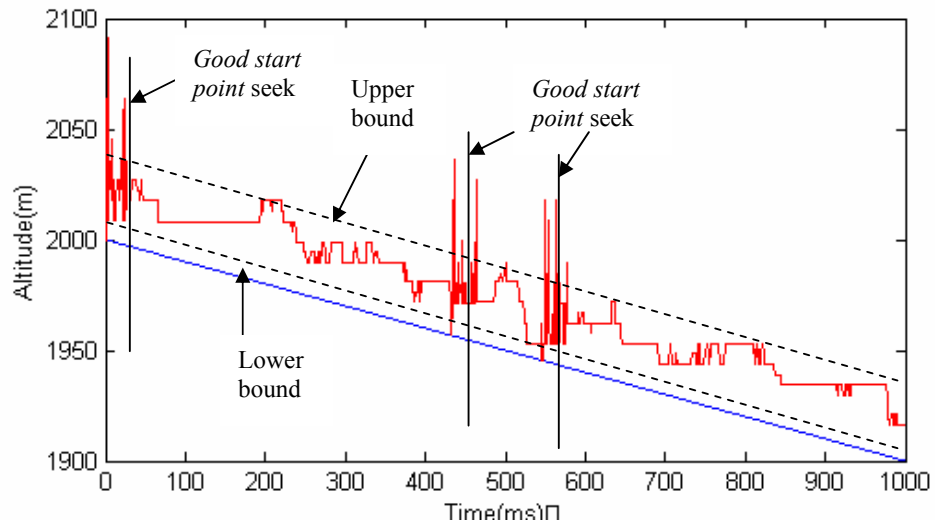
Figure-3.17 Comparison of entered and measured heights for *n*=32. Terrain is sea state-5.
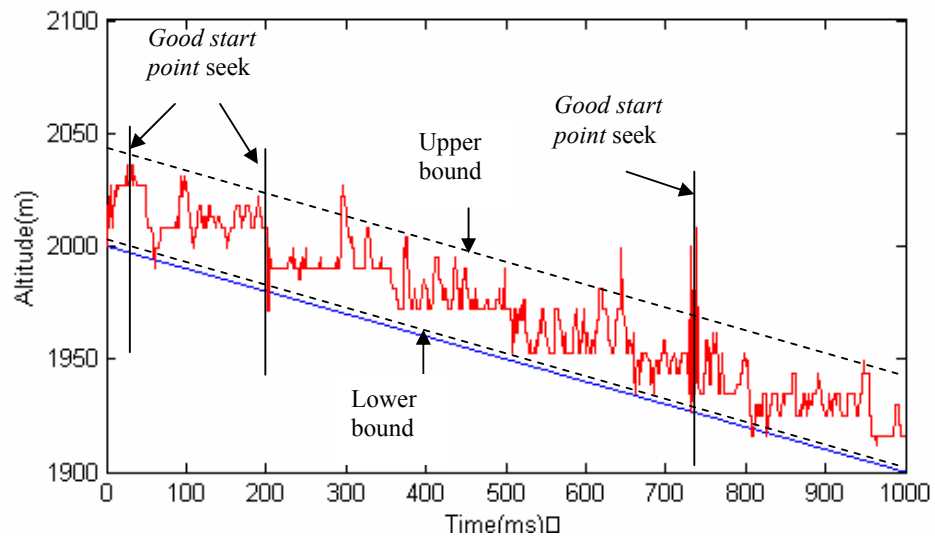
Figure-3.18 Comparison of entered and measured heights for *n*=16. Terrain is sea state-5.

44
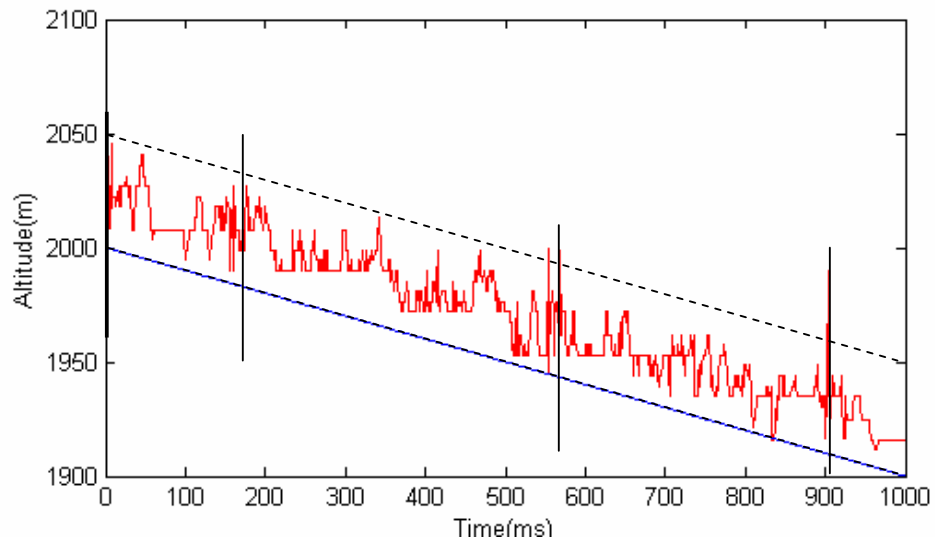
Figure-3.19 Comparison of entered and measured heights for n=8. Terrain is sea state-5.
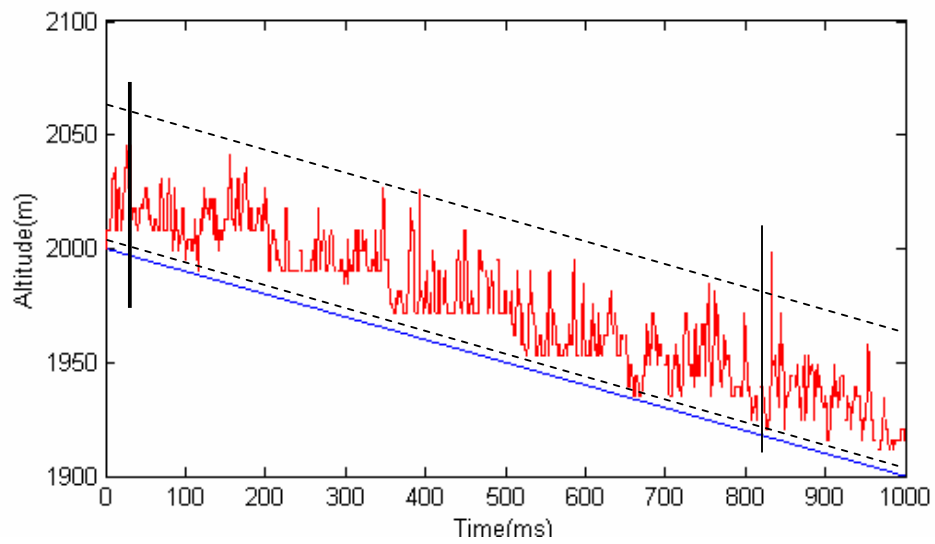
Figure-3.20 Comparison of entered and measured heights for n=4. Terrain is sea state-5.

Figure-3.21 shows the operation of Trimod6 in Windows. This is a bad case, probably more than half of the measurements are missed (out of detect) and algorithm tries to adjust threshold by checking maximum power in the received signal.
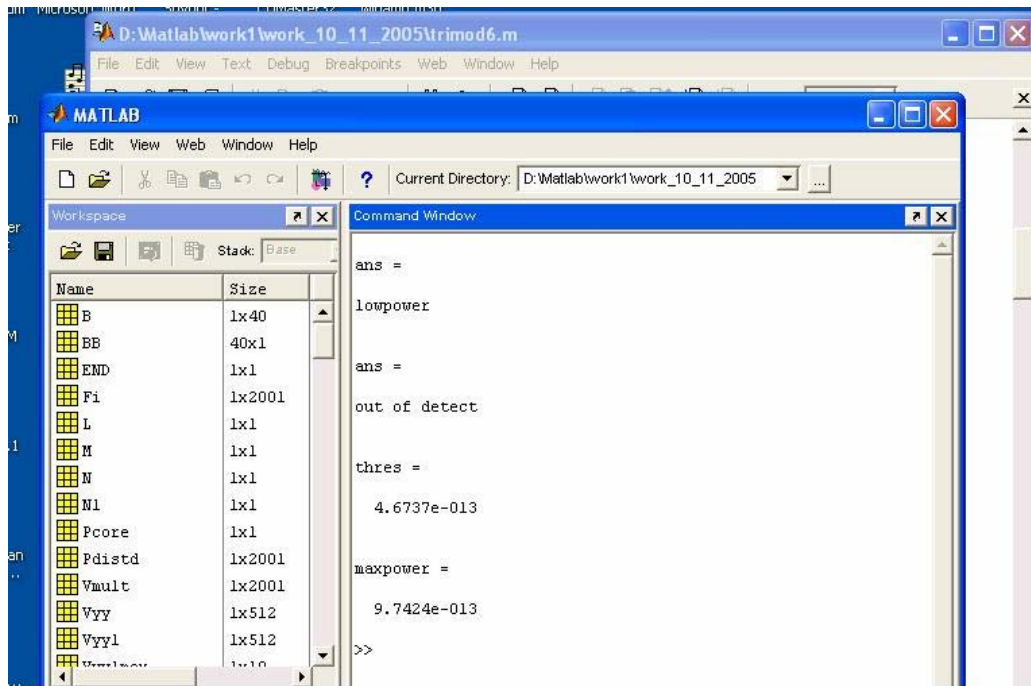
Figure-3.21 Operation of Trimod6 in Windows.

CHAPTER 4

SYSTEM DESIGN

Design of an FM-CW radar altimeter requires attention to many of the factors mentioned before. However this is necessary yet, not adequate for system design. Attention must also be paid to hardware and software of the system to realize it. Operation of concept must be proved. System must operate properly in order to measure and detect range accurately.

Below is a summary of the block diagram of operational FM-CW radar altimeter (Figure-4.1) which is implemented by Tapasan Design Group in Middle East Technical University (METU). The system is created for military and commercial purposes hence some of the important parameter such as RF circuit details, operating voltages and part numbers of integrated circuits are not given.
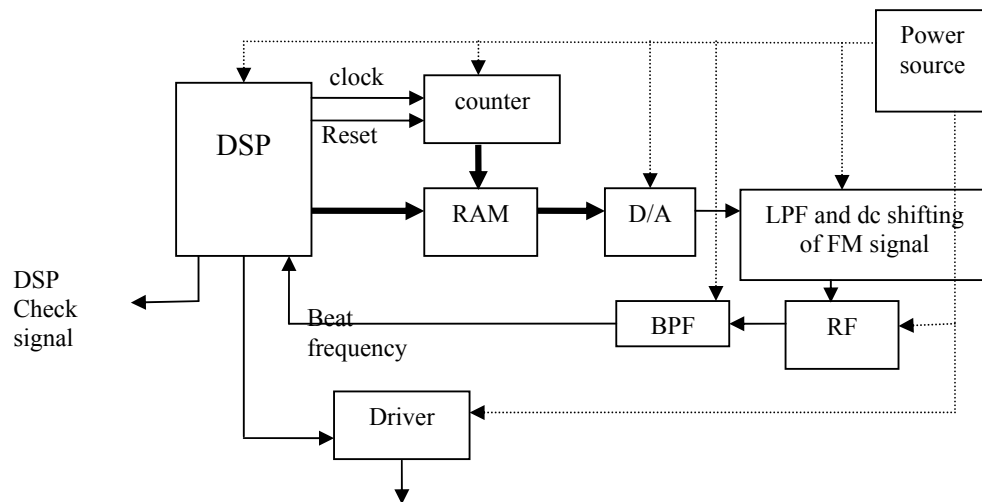
Figure-4.1 Block diagram of the FM-CW radar altimeter.

Briefly, the system operates as follows: The RF circuit transmits FM-CW signal and generates mixed signal with the received and transmitted signals that is necessary for range calculation (Figure-4.2). Mixed signal is band pass filtered (Figure-4.3) so the weak echo is significantly amplified and filtered. The signal is sampled by DSP processor (Figure-4.4) and processed to obtain the desired range. To synchronize process, at the same time modulating signal is generated and fed to RF circuit by DSP processor. Power levels and proper operation of processor is supervised and necessary signal is generated for the driver circuit whenever the threshold is exceeded for the desired range.
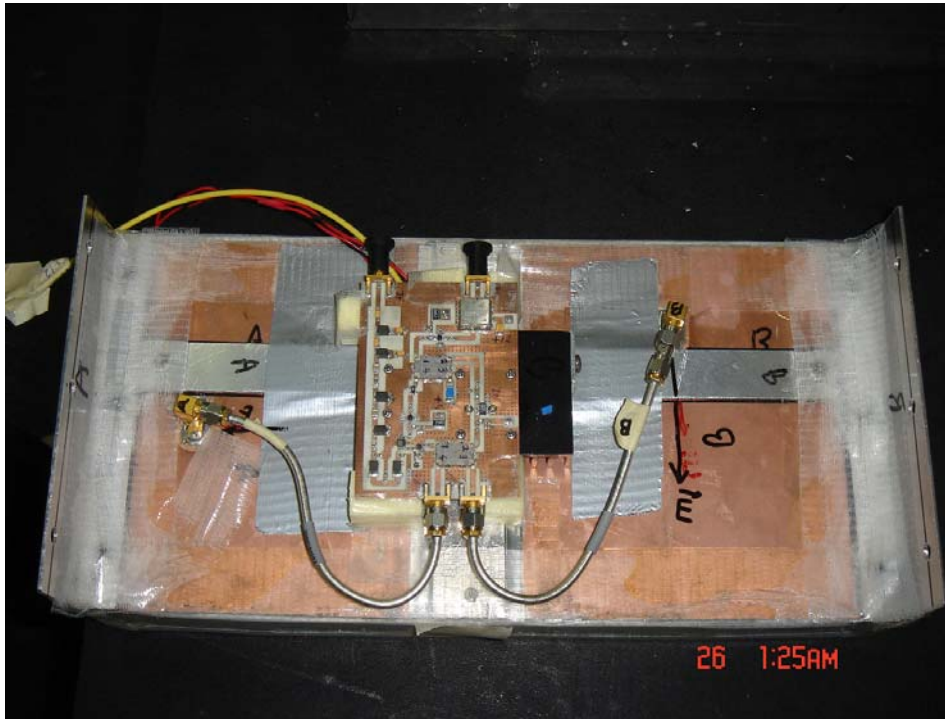
Figure-4.2 Antenna and RF electronic circuits of the FM-CW radar altimeter.
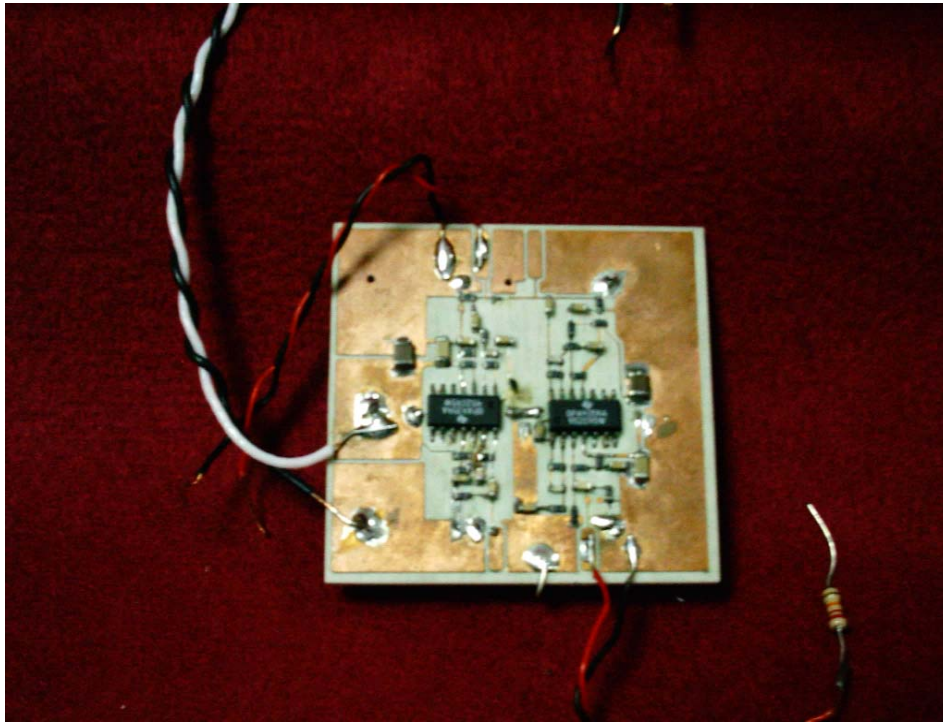
Figure-4.3 A photograph of the band pass filter.
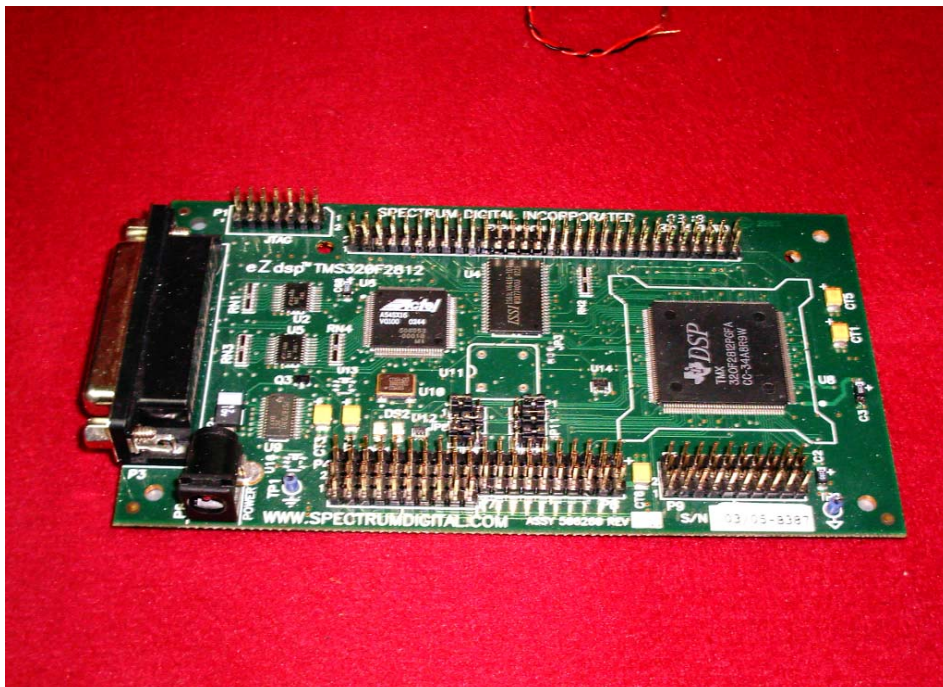
Figure-4.4 A photograph of the DSP processor and digital electronic circuits.

4.1   Design Objectives

The goal of the design is to detect ranges between 150-350 m with a DSP processor, calculation capacity of 150 million multiplications per second. Maximum Δf of FM-CW radar is around 40 MHz.

4.2   RF, Video and Digital Electronics

RF part is composed of a voltage controlled oscillator (VCO), a mixer, low noise amplifiers (LNA), a directional coupler, a circulator and an L-C filter (Figure-4.5). For maximum range resolution referring to (2.32), VCO is operated at maximum Δf.

Output of RF block is fed to band pass filter. Band pass filter is of the type Butterworth. The cut-off frequencies are adjusted for 150 m and 350 m. Gain of the filter is adjusted around 80-100 dB. The gain is adjusted assuming, grazing angle is at near vertical over a large surface.
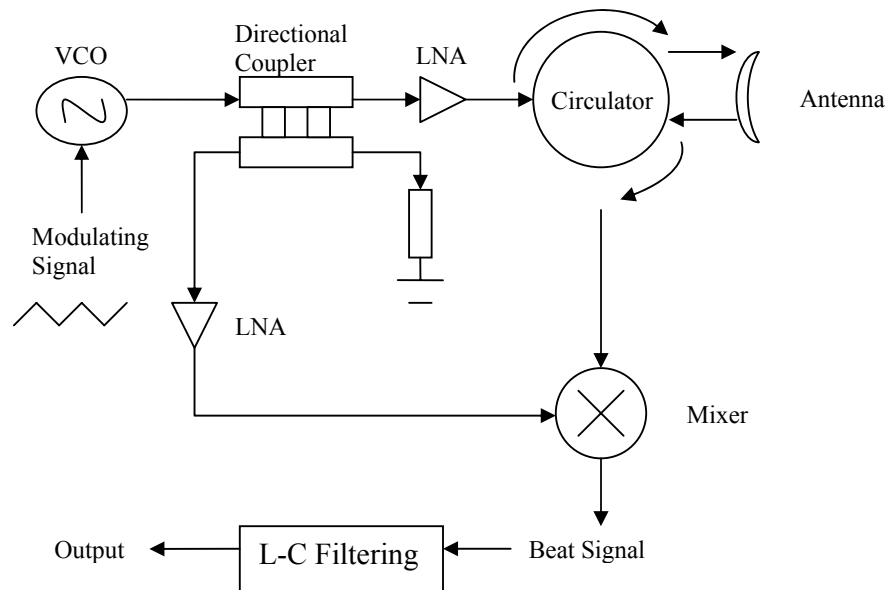
Figure-4.5 RF block diagram.

Digital electronics involve a high speed DSP based Harvard structured processor. The processor is operated at 150 MHz. Additional integrated circuits, memory and digital to analog (D/A) converter are used for modulating signal generation. Selection of f_m of the modulating signal is related with processor speed, range resolution, relative speed of radar and target. Even the leakage coupled from the transmitter to mixed signal is effective on the selection of f_m.

4.3   Processing and Detection Algorithm

Processing parameters are selected with system resources as described in Chapter 2 for design objectives. Δf is selected as 40 MHz and ΔR can be calculated from (2.32) as 3.75 m. Comparison of minimum distance with ΔR reveals that uncertainty in measurement is ± 1.25 %. Combination of (2.29), (2.31), and (2.32) leads to N = 186 for the maximum range of 350 m. To be on safe side and convenient with digital processing N is chosen as 256. For N=256, maximum allowable range is 480 m.

Assume that maximum relative speed of FM-CW radar is 300 m/s and window size is 16 and ΣR is selected as 3 m then referring to Chapter 3, f_m is 800 Hz. From f_m, K can be calculated as 426.7 Hz/m. For N=256 and f_m 800 Hz, f_s is calculated as 409.6 kHz.

K value can be used to verify calculations. For maximum range of 350 m f_{bmax} is 149 kHz. From sampling theorem f_s must be at least 298 kHz which is smaller than selected f_s for safety. Also cut-off frequencies of Butterworth filter can be calculated with K as 64 kHz and 149 kHz.

After FFT, threshold crossing beat frequencies are placed in a 16 slot window. As soon as the window is filled, it is slid and old values are deleted and new values are placed as FIFO. Each time the window is slid values are re-ordered in a buffer and median value is chosen (order statistics) as the detected frequency, hence the range. If the detected range is around the desired range appropriate signal is sent to driver.

4.4 Performance

Since the operation of system from a plane over land or sea is not available yet, FM-CW is operated with a surface acoustic wave (SAW) delay line. Much information on SAW can be obtained from [10]. With the help of SAW delay line and active devices land reflection power and delay is simulated. Simulated range is 427 m and received beat frequency is182 kHz. Receive power level is around -80 dBm and noise level is around -90 dBm.

Although it was beyond the limits of design, experiments showed that most of the time adjusted range is detected by the processor. Seldom interference and noise problems occurred since the received echo (beyond design range) was very weak and out of band of filter. Also the sampling was at limits. Even though, the system successfully operated.

Despite the good results, it is always better to make experiment on the field. Since the spread of spectrum due to many scatterers, Doppler frequency and RCS fluctuations are not included in this experiment.

CHAPTER 5

CONCLUSION

Throughout this thesis, the reader is first informed about the radars, FM-CW radars and radar related physical happenings. After brief information on radars, methods of signal processing and determination of FM-CW radar parameters are discussed.

Later in the Chapter 3, the analytical work created for the simulation of FM-CW radar altimeter is presented. This work is a Matlab code and improved step by step. And results of each step presented throughout Chapter 3. Later the developed algorithm is introduced and the performance is evaluated for different scenarios. With these scenarios more detailed results are obtained about the system. The measured heights and entered heights into simulator are compared. Results and improvements are discussed for different power and noise levels for altitudes between 500 m and 2000 m. Relation between range and detection probabilities and false alarms also investigated and performance improvement parameters are identified with order statistics. Additional methods other than order statistics can also be used such as averaging between FFT power spectrums. Also Wiener filtering can be used for tracking abilities. But amongst all methods, order statistics is the simplest (minimum system resources) yet an effective method for accurate altitude determination.

Next in Chapter 4, implementation of an FM-CW radar altimeter is introduced. This is a physical system and fully operated in laboratory conditions. Selection of system parameters are discussed for real system, block diagram and operation of the system is given.

At overall, some clues are obtained about the operation of the FM-CW radar altimeter. The altimeter is not operated on the field therefore possible outcomes of measurements are generated and evaluated in the computer. From this evaluation, power levels and other parameters are estimated for different scenarios.

And finally for the future work, the simulator must be improved to handle more cases, more accurately. Some of the necessary improvements are:

1. Improvement on antenna pattern. A constant antenna pattern is used for the simulation. But instead a Gaussian approximation or another mathematical model would be more appropriate. This can easily be calculated and implemented into simulator (Appendix B).

2. Improvement of the impulse response for the surfaces with slope and different grazing angles other than near vertical.

3. Addition of lognormal distribution to available distributions.

4. Automatic adjustment of f_m, hence finer measurement results for low altitudes. To increase the maximum range with the available processing capabilities, f_m must be decreased. Decreasing f_m degrades K and decreases measurement time and range resolution for the relative speed case. Hence to increase the performance for low altitudes and relative motion f_m can be adjusted automatically.

5. Finer adjustment of threshold with change in altitude. Since the relative altitude is recorded by the algorithm threshold can be adjusted periodically with relative altitude information. For example if the altitude changes more than a specified value then the threshold is re-adjusted and the relative altitude information is cleared and recorded again.

REFERENCES

[1] Introduction to Radar Systems

   Merrill I. Skolnik, Second Edition, New York McGraw-Hill, 1981.

[2] History of Radar,

   http://www.answers.com/topic/history-of-radar, visited on December 2005.

[3] Radar Basics,

   http://www.itnu.de/radargrundlagen/geschichte/hi05-en.html, visited on
   December 2005.

[4] The Long Quest

   Sandretto, P. C, IRE Trans., vol. ANE-1, no.2, p.2, June 1954.

[5] On Some Direct Evidence for Downward Atmospheric Reflection of Electric
Rays

   Appleton, E. V., and M. A. F. Barnett, vol. A109, p.621, 1925.

[6] A Terrain Clearance Indicator

   Espenshied, L., and R. C. Newhouse, Bell Sys. Tech. J., vol.18, p. 222-234,
   1939.

[7] Fundamentals of Short-Range FM Radar

   Igor V. Komarov, Sergey M. Smolskiy, Artech House, September 2003.

[8] Waveform design principles for automotive radar systems

   Rohling, H. Meinecke, M.-M CIE International Conference on, Proceedings
   p.1-4, October 2001.

[9] Microwave Interaction with Snowpack Observed at the Cold Land Processes Field Experiment

G. Koh, N. D. Mulherin, J. P. Hardy R. E. Davis, and A. Twombly, 59th Eastern Snow Conference Stowe, Vermont USA, 2002.

[10] FM-CW Radar Altimeter Test Board

Aydın Vural, Ms. Thesis, Electric and Electronics (EE) Department at METU, December 2003.

[11] Platform Yaklaşım Radarı Sinyal İşleme Bölümü Algoritma Tanımlama Dokümanı

Ülkü Çilek, Technical Report, Tapasan A.Ş, December 2004.

[12] Radar Reflectivity of Land and Sea

Maurice W. Long, Lexington Books, 1975.

[13] Radar Range-Performance Analysis

Lamont V. Blake, Artech House Inc., 1986.

[14] The Average Impulse Response of Rough Surface and Its Applications

Gary S. Brown, IEEE Transactions On Antennas And Propagation, Vol. Ap-25, No. 1, p.67-73, January 1977.

[15] Radar System Analysis and Modelling

David K. Barton, Artech House, 2005.

APPENDIX A

RADAR FREQENCIES

Table-A.1 Radar frequencies.

Band	Nomenclature	Frequency	Wavelength
ELF	Extremely Low Frequency	3 - 30 Hz	100,000 - 10,000 km
SLF	Super Low Frequency	30 - 300 Hz	10,000 - 1,000 km
ULF	Ultra Low Frequency	300 - 3000 Hz	1,000 - 100 km
VLF	Very Low Frequency	3 - 30 kHz	100 - 10 km
LF	Low Frequency	30 - 300 kHz	10 - 1 km
MF	Medium Frequency	300 - 3000 kHz	1 km - 100 m
HF	High Frequency	3 - 30 MHz	100 - 10 m
VHF	Very High Frequency	30 - 300 MHz	10 - 1 m
UHF	Ultra High Frequency	300 - 3000 MHz	1 m - 10 cm
SHF	Super High Frequency	3 - 30 GHz	10 - 1 cm
EHF	Extremely High Frequency	30 - 300 GHz	1 cm - 1 mm

Table-A.2 Microwave frequencies.

ITU Band	Frequency
VHF	138 - 225 MHz
UHF	420 - 450 MHz 890 – 942 MHz
L	1.215 - 1.400 GHz
S	2.3 - 2.5 GHz 2.7 - 3.7 GHz
C	5.250 - 5.925 GHz
X	8.500 – 10.680 GHz
Ku	13.4 - 14.0 GHz 15.7 - 17.7 GHz

APPENDIX B

ANTENNA PATTERNS

Figure-1.B shows the antenna pattern used for the simulation. The gain is constant within the beam width and zero out side. This simplified antenna pattern can be improved as in Figure-B.2 with Gaussian approximation $A \cdot e^{-2 \cdot \sin(\theta) \cdot \sin(\theta) \cdot b / a}$.
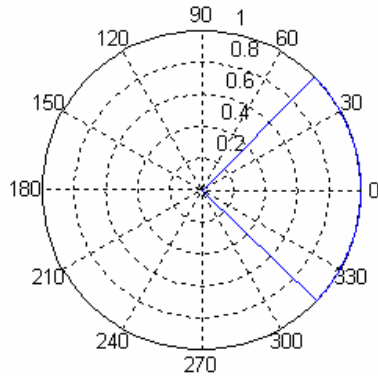
Figure-B.1 Antenna pattern used for the simulation.

(a)   (b)
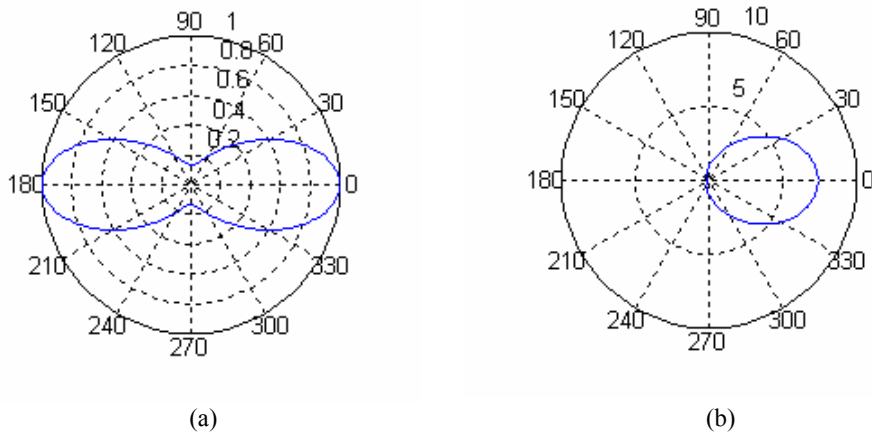
Figure-B.2 Possible antenna patterns. (a) and (b) are Gaussian approximations with different parameters.

APPENDIX C

FLOWCHART OF ALTITUDE DETERMINING ALGORITHM

Figure-C.1, Figure-C.2, and Figure-C.3 shows the flow of the algorithm. Figures are connected with arrows.
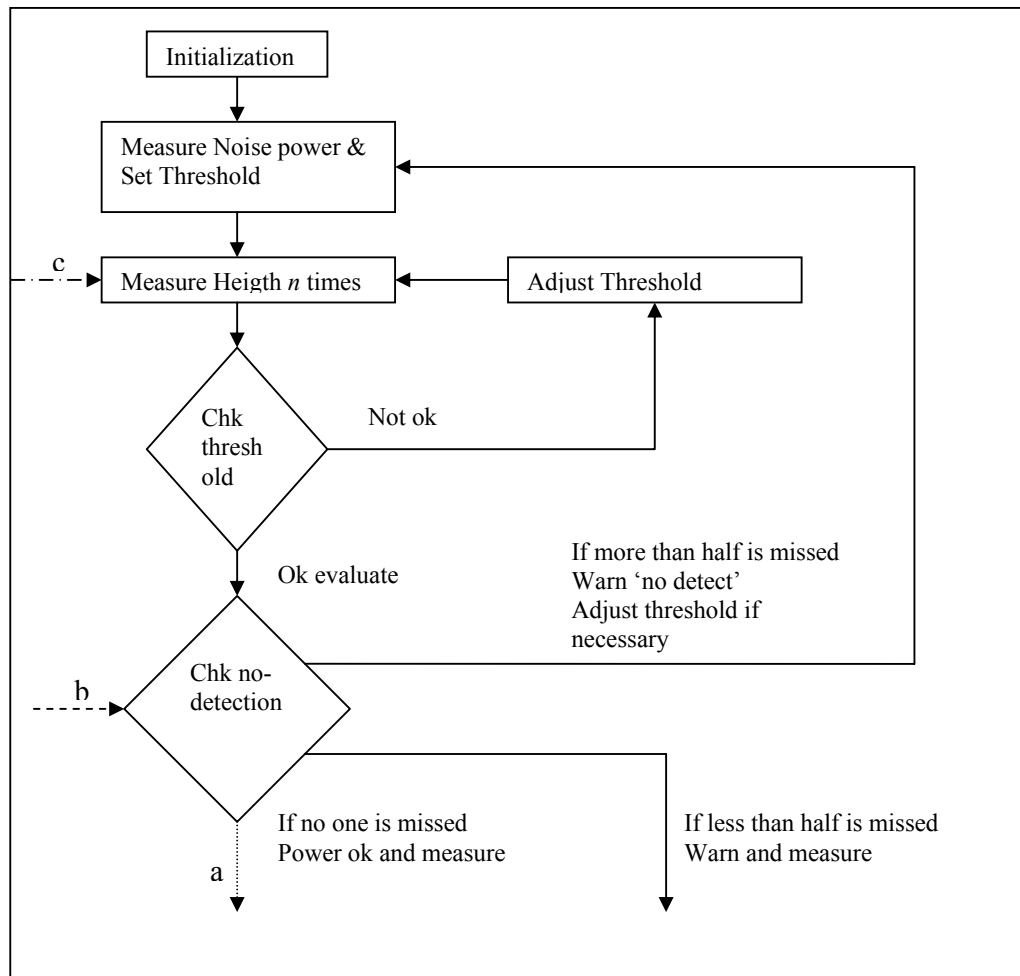
Figure-C.1: Flowchart-1 of altitude determining algorithm.

a

Chk std

Ok → Median fitler size n window, 'power ok' show result Make new measurement and update window. Record delta h

b

Not ok

Warn show result, adjust std limits if necessary. Recall delta h and adjust threshold accordingly.

c
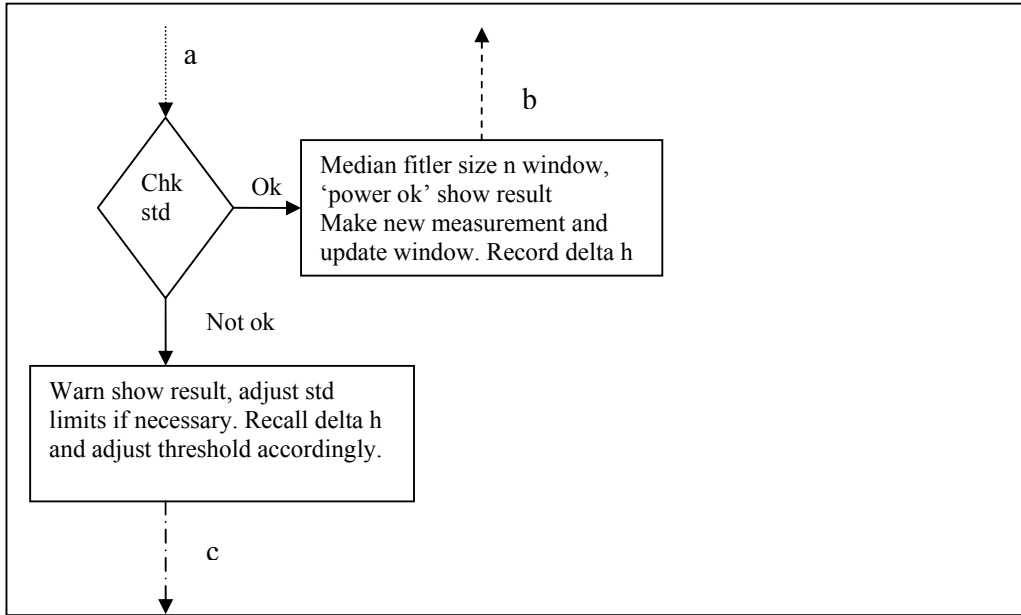
Figure-C.2: Flowchart-2 of altitude determining algorithm.

Chk std

Ok → Warn, 'low power' Copy valid data, median fitler and display results, adjust threshold if necessary. Make new measurement update window-n

b

Not ok

Warn, 'low power' 'out of detect', adjust threshold if necessary

c
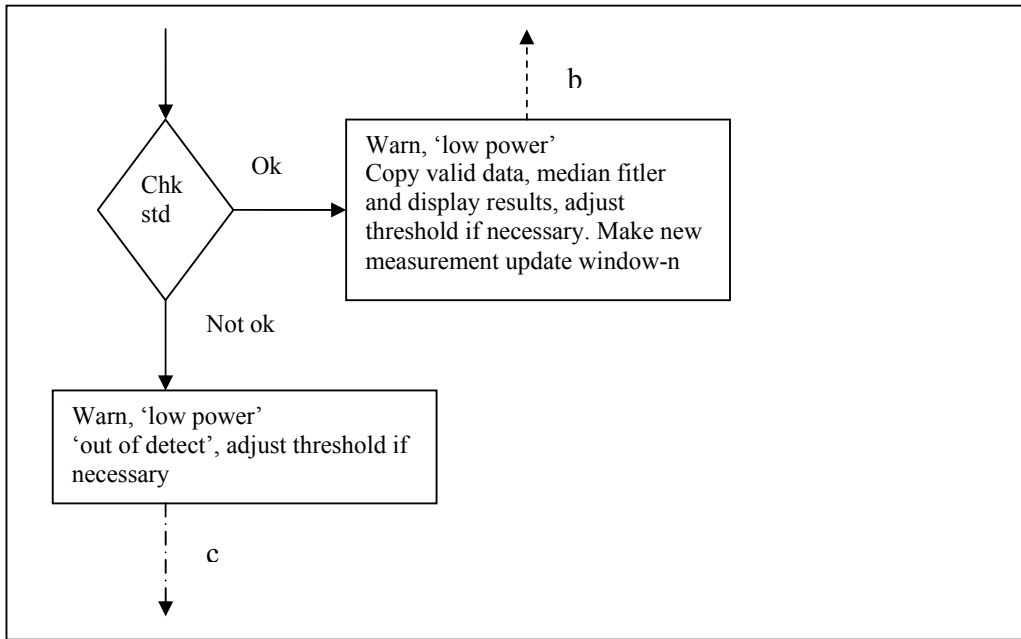
Figure-C.3: Flowchart-3 of altitude determining algorithm.

APPENDIX D

MATLAB CODE USED FOR SIMULATIONS

Trimod6.m

```
%initialize vectors and memory
clear BB;
clear B;

clear havg;
clear hmes;
clear Vyy1max;

clear mem1;
clear mem2;
clear mem3;
clear mem4;
clear mem5;
clear mem6;

%read RCS values from excell to generate curve
BB = xlsread('testdatam1.xls');
B = BB';

%Program control parameters

flucparam = 0;   %0 for rayleigh, 1 for weibull
vargs = 1;       %rayleigh variance parameter
expweib = 1;     %expected value for rt^2 where rt is weibull dist
weiba = 1;       %weibull parameter a
weibb = 2;       %weibull parameter b,b=2 raylegih dist.
```

%weib pdf

%P(x)=a.b.x^(b-1).e^(-a.x^b)

%below are some tabulated values of E(rt^2)
%   b:
%   1.81   1.6   1.4
%   --------------------
% 1 | 1.15   1.42   1.74
%a: 1/2 | 2.46   3.38   4.6
% 1/4 | 5.28   8   12.1

g = 5;   %trasmitted power multiplier_sqrt(10.^(0.5*(g-5)));
wgnpower=-85;   %wgn power in dBm within band of interest
tray = 10;
deltaR =30;
rcs_prm1 = 10.^-2;   %gamma parameter for RCS -40dB for sea state3,roads
                          % -30 dB for sea state5, -20_-10 for grass,
                          %-15db(0.032) for woods, 0dB for urban
rcs_prm2 = 10;   %Average values for near vertical reflection
rsc_prm3 = 0.2;   %2 Decrease,3 Increases with increasing surface roughness

%FMCW parameters

m = 1;
b1 = 0;
b2 = 8e6;
b3 = -16e6;
a1 = 16e9;
a2 = -16e9;
a3 = 16e9;
N = 1024;
N1 = 512;
samplingperiod = 1e-7;
mult=1/samplingperiod;
dsmp = 10;
dsmp1 = 10;
dsmp2 =10;
devam = 1;
casenuma = 1;
integh=0;
no = 0;

```
hfile;
hcount=1;

while devam == 1
    switch casenuma
    case 1
        % measure noise level and set threshold;
        Pcore = 0;
        h = hu(hcount);
        hmes(hcount)=h;
        hcount = hcount+1;
        measure;
        minthres = 20*sum(Vyy1)/N1;
        thres = minthres
        %plotfigure
        casenuma = 2;
    case 2
        %clear relative heigth measurement
        integh=0;
        flag1 = 0;
        %enable output power
        Pcore = 1;
         %make tray measurements and get heigths
        for q=1:tray
            h = hu(hcount);
            measure;
            Vyy1max(q) = max(Vyy1);
            %plotfigure
            getheigth;
            havg(q) = heavg;
            hmes(hcount)=heavg;
            hcount = hcount+1;
        end
        maxpower = median(Vyy1max)
        if maxpower >= 300*thres
            thres = 10*thres
            casenuma = 2;
        else
            hcount=hcount-1;
            casenuma = 3;
        end
```

```matlab
case 3
    %count number of no detections
    no=0;
    clear loc2;
    loc2count = 1;
    for q = 1:tray
        if isnan(havg(q)) == 1
            no = no+1;
        else
            loc2(loc2count) = havg(q);
            loc2count = loc2count+1;
        end
    end
    if no == 0
        if flag1 == 1
            mem4 = std(havg,1);
            mem5old = mem5;
        else
            mem4 = std(havg,1);
            mem5 = median(havg);
            mem5old = mem5;
        end
        if mem4 <= deltaR
            flag1 = 1;
            clc;
            'power ok'
            hmes(hcount)=round(mem5);
            round(mem5)
            h
            hcount = hcount+1;
            h = hu(hcount);
            measure;
            getheigth;
            slidewin;
            mem5 = median(havg);
            %plotfigure;
            % difference heigth. If heigth increases integh is negative
            %othervise positive
            integh = mem5old-mem5 + integh;
            casenuma = 3;
        else
            clc;
            hmes(hcount)=round(mem5);
            'warning',round(mem5)
            h
            'Change deltaR? Current deltaR is',deltaR
            keyboard
```

64

```
        if integh > 0
            thres = thres*10;
        end
        if (thres > minthres) & (integh < 0)
            thres = thres/10;
        end
        hcount = hcount+1;
        casenuma = 2;
    end
end
if  (0 < no) & (no<=tray/2)
    clc;
    'lowpower'
    stdlow = std(loc2,1);
    heigthlow = median(loc2);
    if stdlow <= deltaR
        hmes(hcount)=round(heigthlow);
        heigthlow
        h
        hcount = hcount+1;
        h = hu(hcount);
        measure;
        getheigth;
        slidewin;
        if  thres > minthres
            thres = thres/10;
        end
        casenuma = 3;
    else
        'out of detect'
        if  thres > minthres
            thres = thres/10;
        end
        hcount = hcount+1;
        casenuma = 1;
    end
end
if no > tray/2
    clc;
    'lowpower'
    'out of detect'
```

```
        if  thres > minthres
            thres = thres/10;
        end
        hcount = hcount+1;
        casenuma = 1;
      end
   end
if hcount == 2800
   devam = 0;
end
end
```

1   measure.m

```
clear yop;
clear you;
clear w;
clear wcut1;
clear wcut2;
clear Vyy1;
clear Vyy2;

% get theoric concentric impulse response
convolve;
% get transmitted wave and its delayed version
TxdelayTx;

%addition of rayleigh type voltage fluctuation
Pmult = Pdistd;
rndgen;

%convolution of impulse response and double rx singnal and resize
yop =conv(y,hat);
you= yop((10000*m) +1:(20000*m));

%mix of tx and rx
w = wagn+you.*yy;

%decomposition of up and down going edges
wcut1 = [w(7125*m+1:10000*m) w(1:2125*m)];
wcut2 = w(2125*m+1:7125*m);

%preprocessing of wcut1;
wcut = wcut1;
dsmp = dsmp1;
clear wcut1;
preproc;
wcut1 = hwcut;
```

```
%preprocessing of wcut2;
wcut = wcut2;
dsmp = dsmp1;
clear wcut2;
preproc;
wcut2 = hwcut;

%take FFT of wcut1
wcut = wcut1;
takefft;
Vyy1 = Vyy;
f1 = freq;
```

1.1   convolve.m

```
clear rt;
clear x;
clear z;
clear y;
clear r;
clear Fi;
clear re;
clear ro;
clear arean;
clear Pdistd;

step = 1;
tetab = pi/6;
tetae = pi/2-tetab;
rmax=floor(h/sin(tetab));
END =floor((rmax-h)/step)+1;
rt = h:step:rmax;
td = 2/3*h*samplingperiod/dsmp2;

x=(pi/2 - tetae):pi/360:pi/2;

%this line is for defined formula
y=rcs_prm1*sin(x)+rcs_prm2*exp(-rsc_prm3*(90-x/pi*180));

%these lines are for different terrain types from excell data
%lim = round(tetae/pi*360);
%z= 0.1*ones(1,(lim-39)); %tetae/pi*180 tam sayi olmali
%y=[z B];
%y=(sin(x)).*y;

r = sqrt(rt.^2-h.^2);
```

```
Fi = asin(h./rt);
Fi = sort(Fi);
ro = interp1(x, y, Fi);
ro = fliplr(ro);

arean = 2*pi.*r;

Pdistd = Pcore*25*0.15*0.15/((4*pi)^3)*ro.*arean./(rt.^4);

%take FFT of wcut2
wcut = wcut2;
takefft;
Vyy2 = Vyy;
f2 = freq;
```

1.2   TxdelayTx

```
clear u;

clear t;
clear t1;
clear t2;
clear t3;
clear t4;
clear z1;
clear z2;
clear z3;
clear z4;
clear z;
clear zz;
clear y;
clear yy;

L  = floor(td/samplingperiod+2e-10);

t1 = 0:samplingperiod:0.00025;
t2 = 0.00025+samplingperiod:samplingperiod:0.0005;
t3 = 0.0005+samplingperiod:samplingperiod:0.00075;
t4 = 0.00075+samplingperiod:samplingperiod:0.001+td;

ta= [t1 t2];
tb= [t3 t4];
t = [ta tb];

z1 = a1*pi*(t1.^2);
z2 = 2*pi*b2*(t2-0.00025) + a2*pi*(t2.^2-0.00025.^2);
z3 = 2*pi*b2*(t3-0.0005) + a2*pi*(t3.^2-0.0005.^2);
z4 = 2*pi*b3*(t4-0.00075) + a3*pi*(t4.^2-0.00075.^2);
```

```
z = [z1 z1(end)+z2 z1(end)+z2(end)+z3 z1(end)+z2(end)+z3(end)+z4];
M=length(z);

clear zz;

for s=1:1:M-L
    zz(s) = z(s+L);
end

zz=zz(1:M-L-1);
z=z(1:M-L-1);

y = cos(z)+j*sin(z);
yy = cos(zz)-j*sin(zz);

y = [y y];
```

1.3   rndgen.m

```
clear a;
clear b;
clear hat;
clear chat;
clear dhat;
clear wagn;
clear Vmult;
clear xt;
clear rot;

if flucparam == 0
        Vmult = sqrt(Pmult*50/2/vargs);
        a=Vmult.*(normrnd(0,vargs,[1,END]));
        b=Vmult.*(normrnd(0,vargs,[1,END]));
        chat=complex(a,b);
        dhat=downsample(chat,dsmp2);
        hat = dhat*sqrt(10.^(0.5*(g-5)));
else
        Vmult = sqrt(Pmult*50/expweib);
        xt = unifrnd(0,2*pi,[1 END]);
        rot = Vmult.*weibrnd(weiba,weibb,[1 END]);
        a = rot.*cos(xt);
        b = rot.*sin(xt);
        chat=complex(a,b);
        dhat=downsample(chat,dsmp2);
        hat = dhat*sqrt(10.^(0.5*(g-5)));
end
```

```
wagn = wgn(1,10000*m,wgnpower,50,'dBm','complex');

clear Pmult;
```

1.4   preproc

```
clear b;
clear a;
clear dwcut;
clear hwcut;
clear fwcut;
clear ham;

[b,a] = cheby2(6,30,5e5/5e6);

fwcut = filter(b,a,wcut);

dwcut = downsample(fwcut,dsmp);
ham = hamming(length(dwcut))';
hwcut = ham.*dwcut;

clear wcut;
clear dsmp;
```

1.5   takefft

```
clear W;
clear Vyy;
clear freq;

W = fft(wcut,N1);
W = fftshift(W);
Vyy = abs(W).^2 / N1/N1;

freq = mult/dsmp1*(-N1/2:(N1/2-1))/N1;

clear wcut;
```

2   getheigth.m

```
clear HH;
clear fif;
clear he1;
clear he1;
clear heavg;
```

```
%get heigth1 from power spectrum of wcut1
HH = fliplr(Vyy1);
fif = fliplr(f1);
heightrslt;
he1 = him/106;

%get heigth2 from power spectrum of wcut2
HH = Vyy2;
fif = f2;
heightrslt;
he2 = him/106;
%get heigth from average of h1 & h2
heavg = (abs(he1)+he2)/2;
```

2.1   heightrslt

```
clear him;
k=N1/2;

while ((HH(k) <= thres) & (k < N1))
      k = k+1;
end

if (k ~= N1)

      him = fif(k);

else

      him = NaN;

end

clear fif;
clear HH;
```

3   slidewin.m

```
clear loc1;
clear q;

for  q = 1:(tray-1)
   loc1(q)=havg(q+1);
end

loc1(tray) = heavg;
clear havg;
havg = loc1;
```

APPENDIX E

EXCEL DATA SHEET USED FOR SIMULATIONS

Table-E.1 shows the data entered as an excel sheet. The data is interpolated in the algorithm and intermediate values are calculated accordingly. Figure-E.1 shows the plot of data in Table-E.1.

Table-E.1 Grazing angle versus RCS values. RCS-1 stands for alfalfa and RCS-2 stands for asphalt runaway respectively.

| Grazing angle (degrees)	21	24	27	30	33	36	39	42
RCS-1 (dB)	0.0251	0.0251	0.0251	0.0251	0.0251	0.0252	0.0252	0.0253
RCS-2 (dB)	0.0003	0.0004	0.0005	0.0007	0.0009	0.0012	0.0016	0.0023
Grazing angle (degrees)	45	48	51	54	57	60	63	66
RCS-1 (dB)	0.0255	0.0258	0.0264	0.0277	0.03	0.0346	0.0435	0.0608
RCS-2 (dB)	0.0032	0.0048	0.0073	0.0114	0.0186	0.0311	0.0531	0.0923
Grazing angle (degrees)	69	72	75	78	81	84	87	90
RCS-1(dB)	0.0941	0.1586	0.2833	0.5246	0.9916	1.8951	3.6431	7.0251
RCS-2(dB)	0.1625	0.2891	0.5178	0.9323	1.6846	3.0518	5.5382	10.063
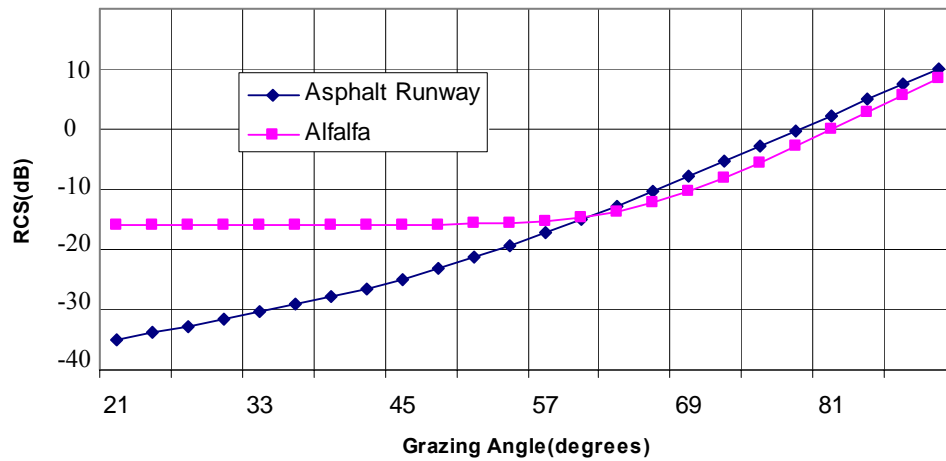
Figure-E.1 Grazing angle versus RCS graph.